European Journal of Medicinal Chemistry 216 (2021) 113333

Contents lists available at ScienceDirect

European Journal of Medicinal Chemistry

journal homepage: http://www.elsevier.com/locate/ejmech

Rational drug design of benzothiazole-based derivatives as potent signal transducer and activator of transcription 3 (STAT3) signaling pathway inhibitors

Dingding Gao [a, c, 1], Nan Jin [b, 1], Yixian Fu [b, d], Yueyue Zhu [a], Yujie Wang [a], Ting Wang [b], Yuehong Chen [b], Mingming Zhang [a], Qiang Xiao [a], Min Huang [b, d], Yingxia Li [a, *]

[a] School of Pharmacy, Fudan University, Shanghai, 201203, China
[b] Division of Antitumor Pharmacology, State Key Laboratory of Drug Research, Shanghai Institute of Materia Medica, Chinese Academy of Sciences, Shanghai, 201203, China
[c] Innovation Research Institute of Traditional Chinese Medicine (IRI), Shanghai University of Traditional Chinese Medicine, Shanghai, 201203, China
[d] University of Chinese Academy of Sciences, Beijing, 100049, China

ARTICLE INFO

Article history:
Received 8 December 2020
Received in revised form
19 February 2021
Accepted 20 February 2021
Available online 2 March 2021

Keywords:
STAT3 signaling pathway
Benzothiazole
Rational design
Antitumor activity
Molecular docking

ABSTRACT

The cumulative evidence supports STAT3, a transcriptional mediator of oncogenic signaling, as a therapeutic target in cancer. The development of STAT3 inhibitors remain an active area of research as no inhibitors have yet to be approved for cancer treatment. In a continuing effort to develop more potent STAT3 inhibitors based on our previously identified hit compound **16w**, a series of benzothiazole derivatives with unique binding mode in SH2 domain of STAT3 were designed, synthesized and biologically evaluated. Of note, compound **B19** demonstrated excellent activity against IL-6/STAT3 signaling pathway with the IC_{50} value as low as 0.067 μM as determined by a luciferase reporter assay. Moreover, multiple compounds displayed potent antiproliferative activity against MDA-MB-468 and *JAK2* mutant HEL cell lines. Further biochemical study using Western blot assay indicated that **B19** blocked the phosphorylation of STAT3 at Tyr 705 and Ser 727 and thus suppressed STAT3-mediated gene expression of *c-MYC* and *MCL-1*. Simultaneously, it induced cancer cell G2/M phase arrest and apoptosis both in MDA-MB-468 and HEL cell lines. Finally, molecular docking study along with surface plasmon resonance (SPR) and fluorescence polarization (FP) assays disclosed the binding mode of **B19** in STAT3 SH2 domain. Taken together, our finding suggests that **B19** is a promising therapeutic STAT3 inhibitor for cancer treatment.

1. Introduction

Signal transducer and activator of transcription 3 (STAT3) is an intracellular latent transcription factor that belongs to STAT protein family [1,2]. It contains six functional domains including a dimerization domain at the N-terminus, a coiled-coil domain for protein-protein interactions, a central DNA-binding domain, a linker domain that affects DNA-binding stability, a classic Src homology 2 (SH2) domain and a carboxyl transactivation domain [2]. Generally, STAT3 transmits signals from the cell surface to the nucleus, as well as directly participates in transcriptional regulation of numerous gene expression [3,4]. Upon triggered by upstream signals, such as various cytokines and growth factors, the Janus kinases (JAKs) are recruited to the receptor and phosphorylate the tyrosine residues on the receptor, creating binding sites for proteins possessing SH2 domains, such as STAT3. The latter can bind to the receptor using SH2 domains and JAKs phosphorylate STAT3 at Tyrosine 705 (Tyr705), which causes STAT3 to dissociate from the receptor. Two activated STAT3 monomers undergo dimerization through reciprocal pTyr-SH2 domain interactions and then translocate into the nucleus to bind specific DNA sequence, leading to target gene transcription [5,6]. Under normal physiological conditions, the activation of STAT3 is rapid and transient due to the negative regulation by proteins such as protein inhibitor of activated STAT (PIAS) and suppressor of cytokine signaling (SOCS) [7–9]. Nevertheless, aberrant activation of STAT3 has a contributing role in diverse solid and hematological tumors as it is a point of intersection of multiple oncogenic signaling pathways [10–14].

* Corresponding author.
E-mail address: liyx417@fudan.edu.cn (Y. Li).
[1] These authors contributed equally to this work.

https://doi.org/10.1016/j.ejmech.2021.113333
0223-5234/

Additionally, STAT3 plays a crucial role in immune cells and is being regarded as a potent immune checkpoint that mediates tumor-induced immunosuppression from various perspectives [15–19]. As STAT3 is the main mediator of IL-6 signaling pathway in Th17 cells, it also plays an important role in pathogenesis of autoimmune diseases, such as inflammatory bowel disease and rheumatoid arthritis [20,21]. Some other studies further showed that different subcellular localization patterns of STAT3 affected autophagy in various ways [22]. Therefore, the discovery of potent STAT3 inhibitors is of great significance for the treatment in many diseases, especially cancer [23].

So far, a variety of STAT3 inhibitors containing peptide, peptidomimetic, small molecule and small-molecule degrader have been reported (Fig. 1) [24–28], which target the SH2 domain or DNA-binding domain to inhibit STAT3 transcriptional activity. However, there are only three small-molecule STAT3 inhibitors (BBI608, OPB-111077, C188-9) currently under investigation in clinical trials, perhaps due to the complexity of the biological functions of STAT3 signaling pathway or the poor physicochemical properties of STAT3 inhibitors. In detail, BBI608 (Napabucasin), a direct STAT3 inhibitor that blocks stem cell activity in cancer cells, is the only STAT3-targeted agent that has been advanced into phase III trials for the treatment of a variety of cancers [29]. OPB-111077, a novel inhibitor of STAT3 and mitochondrial oxidative phosphorylation, is investigated in phase I trial in unselected advanced cancers (NCT01711034) [30]. C188-9, an oral STAT3 inhibitor targeting SH2 domain, is evaluated in phase I trial in the patients with advanced cancers (NCT03195699), which is also under development for the treatment of fibrosis and inflammation [31]. Overall, the discovery of novel potent STAT3 inhibitors remains to be further explored and developed.

In our previous study, molecular docking-based virtual screening was applied to discover a STAT3 inhibitor with a benzothiazole scaffold targeting the Leu706-Phe 710 binding site of the STAT3 SH2 domain. Further investigation showed that compound **16w** exhibited potent inhibition of IL-6/STAT3 signaling with an IC_{50} value of 1.6 μM as determined by a luciferase reporter assay [32]. With the aim of obtaining more potent STAT3 signaling inhibitors, rational drug design based on **16w** was carried out in this study. Among those designed compounds, **B19** exhibited the most potent inhibitory activity towards IL-6/STAT3 signaling pathway, which was 24-fold more potent than hit compound **16w** according to the IC_{50} values (0.067 μM vs 1.6 μM). Moreover, it displayed potent *in vitro* antiproliferative activities against MDA-MB-468 cells and HEL (*JAK2* V617F) cells, through inhibiting STAT3 signaling pathway.

2. Results and discussion

2.1. Design

Firstly, molecular docking of **16w** with STAT3 SH2 domain was conducted using the X-ray crystal structure of STAT3/DNA complex (PDB code: 1BG1), and the proposed binding mode was depicted in Fig. 2A and B. For Fig. 2A, three hydrogen bonds were formed between compound **16w** and the amino acid residues Gln644, Glu638 and Gln635 of STAT3 protein (Fig. 2A). As shown in Fig. 2B and C, a hydrophobic cleft (S1) enclosed by the Phe716, Trp623, Ile659 residues was located near the ring A and various substituents with different sizes or electrical properties could be introduced to explore the inhibitory activities (compounds **B1**–**B14**, **B17**, **B18**). The aromatic ring B inserted into a hydrophobic pocket (S2) surrounded by Met648, Tyr640, Ile653, Ile711 residues and hydroxy or methoxyl was incorporated to form hydrogen-bond or hydrophobic interaction to improve the activities (compounds **B19**–**B23**). We also investigated the effect of chiral methyl group or the long alkyl chain (compounds **B15**, **B16, B24**–**B30**) or thioether bond (**B31**, **B32**) on the activity of STAT3 signaling pathway (Fig. 2C).

2.2. Chemistry

To obtain benzothiazole-based derivatives **B1**–**B17**, a modified literature method was used (Schemes 1 and 2) [32]. Intermediate **2** was prepared from commercially available (S)-1 phenylethan-1-amine and 2-chloroacetyl chloride using triethylamine in 90% yield. Then it was condensed with 6-aminobenzothiazole-2-thiol in refluxing acetone to afford the key intermediate **3** in almost quantitative yield without affording N-nucleophilic addition byproduct. Treatment of the substituted 4-hydroxybenzoic acids (**4a**-**4n**) or **7b** with 2-bromopentane and potassium hydroxide in ethanol at 78 °C resulted in the formation of **5a**-**5n** or **8c** in about 50–80% yield. The intermediates **8a** and **8b** were prepared by Mitsunobu reaction among the appropriate substituted alcohols with **7a** in 38.9% and 64.0% yields respectively [33]. Then, compounds **8a**-**8c** were conveniently hydrolyzed to provide the corresponding acid **9a**-**9c** quantitatively. The benzoyl chloride derivatives (**6a**-**6n**, **10a**-**10c**) were prepared from corresponding benzoic acids (**5a-5n**, **9a-9c**) reacted with $SOCl_2$. Subsequently, target compounds **B1**–**B17** were obtained, respectively, by the reaction between **3** and the corresponding acyl chloride (**6a-6n, 10a-10c**) in the presence of potassium carbonate at room temperature in dichloromethane (36.7–82.7% yields).

The synthetic route for compounds **B18**–**B26** was shown in Scheme 3. Formylation of 2-methylbenzene-1, 3-diol (**15**) with

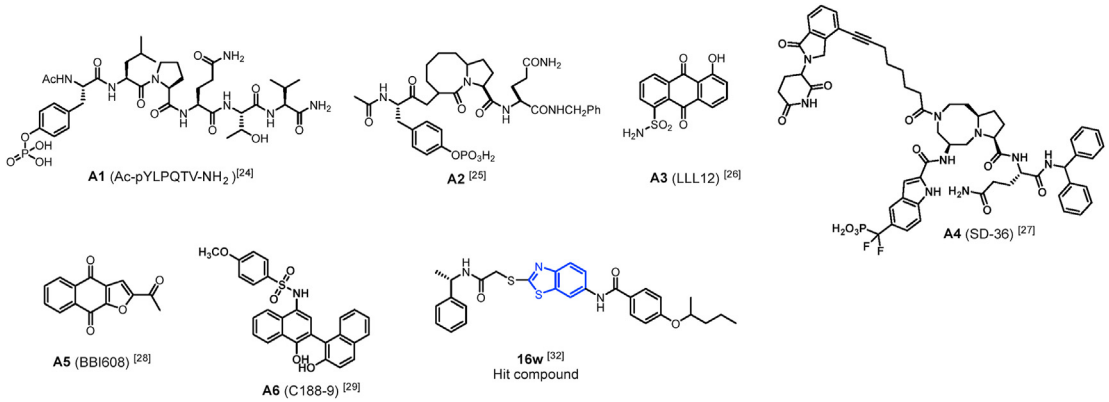

Fig. 1. Known representative STAT3 inhibitors.

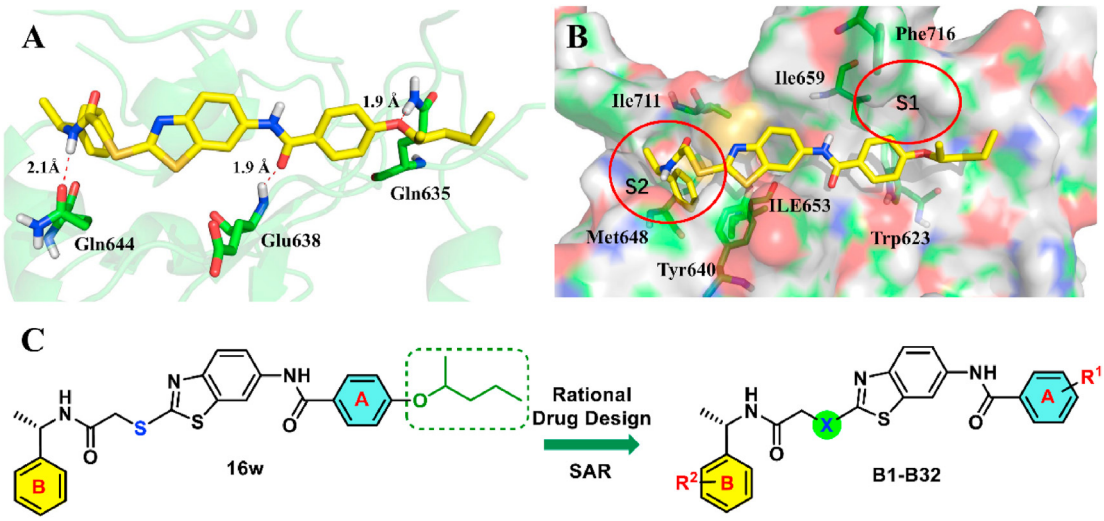

Fig. 2. (A–B) Docking mode of hit compound **16w** with STAT3 SH2 domain (PDB 1BG1), generated by Schrodinger, Maestro suite. Surface representation was created with PyMOL Viewer. (C) Rational design of target compounds.

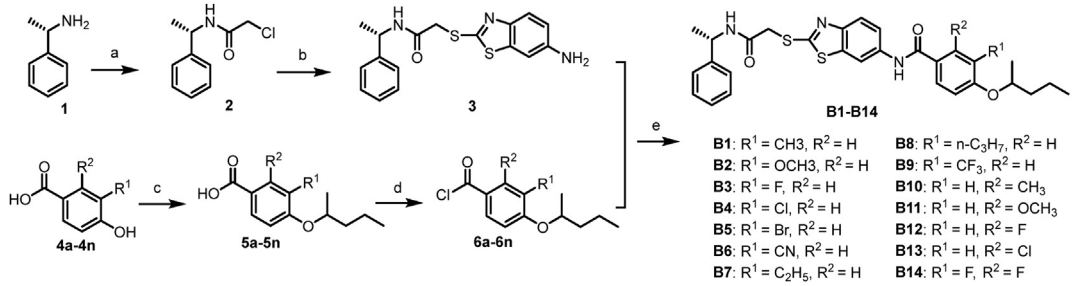

Scheme 1. Synthesis of compounds **B1**–**B14**. Reagents and conditions: (a) $ClCH_2COCl$, Et_3N, CH_2Cl_2, 0 °C to rt; (b) 6-aminobenzothiazole-2-thiol, K_2CO_3, acetone, reflux; (c) 2-bromopentane, EtOH, KOH, reflux; (d) $SOCl_2$, reflux; (e) K_2CO_3, CH_2Cl_2, rt.

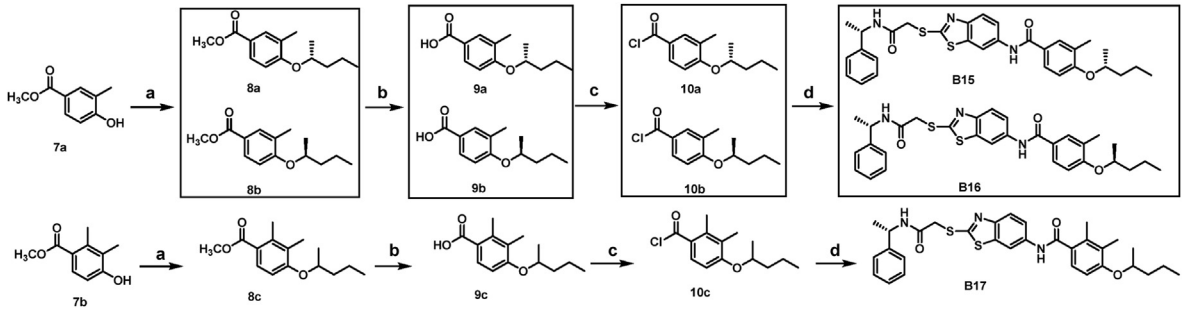

Scheme 2. Synthesis of compounds **B15**–**B17**. Reagents and conditions: (a) **8a**: (*S*)-pentan-2-ol, triphenylphosphane, DEAD, THF, 0 °C to rt; **8b**: (*R*)-pentan-2-ol, triphenylphosphane, DEAD, THF, 0 °C to rt; **8c**: 2-bromopentane, EtOH, KOH, reflux; (b) 1 M NaOH (aq.), rt; (c) $SOCl_2$, reflux; (d) **3**, K_2CO_3, CH_2Cl_2, rt.

$POCl_3$–DMF regio-selectively afforded the benzaldehyde derivative **16** in an excellent yield. Sequential O-alkylations were performed in the DMF to afford **17a**-**17c** in 60.0–75.0% yields [34,35]. After O-methylation of compounds **16** and **17a**-**17c**, oxidation was carried out under $NaClO_2/NaH_2PO_4{\cdot}2H_2O$ buffer solution (pH = 4.5) to provide **19a**-**19d** in 63.1–83.0% yields. The intermediates **13b**-**13d** were obtained after demethylation by BBr_3 (17% in CH_2Cl_2). Condensation of the amines (**14a**-**14e**) with benzoyl chloride derivatives (**20a**-**20d**), which were prepared from the corresponding carboxylic acid (**19a**-**19e**) and $SOCl_2$, provided the desired compounds **B18**–**B26** in 18.0–70.4% yields (Scheme 3).

Synthesis of compounds **B27**–**B30** was depicted in Scheme 4. After selectively protecting one hydroxyl of the starting material **21** with benzyl (**22**), the remaining hydroxyl group was methylated with iodomethane to get compound **23** in almost quantitative yield. Then compound **26** was obtained by oxidation of the aldehyde group, removal of the benzyl group, and methylation of carboxyl group sequentially in a good yield. Subsequent alkylation of **26** under several conditions afforded compounds **27a**-**27d** in 41.9–93.5% yields [36–40], which were hydrolyzed under 1 M NaOH and CH_3OH solution to afford **28a**-**28d** quantitatively. Finally, the carboxyl was converted to acyl chloride group (**29a**-**29d**) and condensed with the amino group of **14a** to obtain compounds **B27**–**B30** in 30.0–35.0% yields.

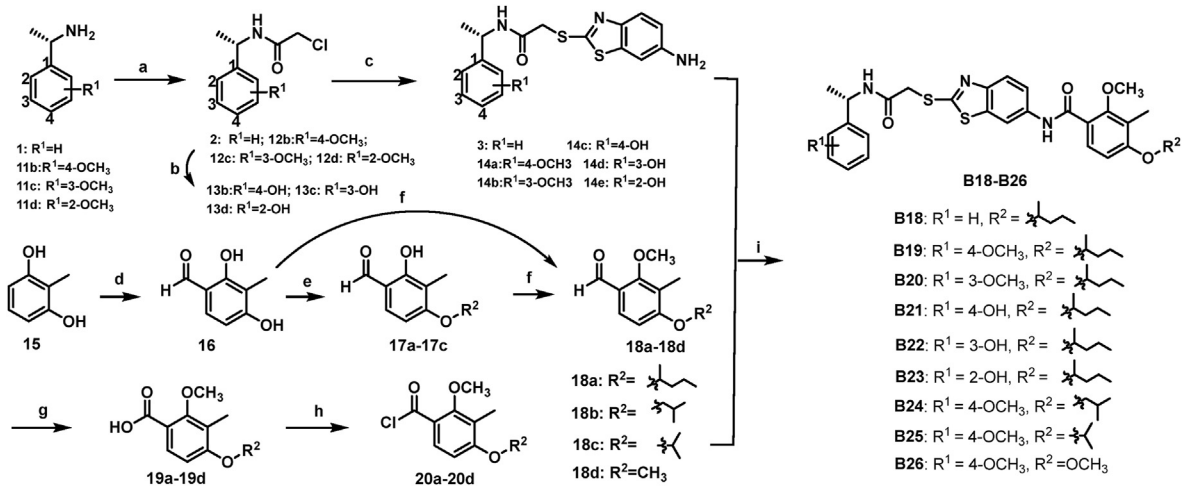

Scheme 3. Synthesis of compounds **B18**–**B26**. Reagents and conditions: (a) 2-chloroacetyl chloride, K_2CO_3, CH_2Cl_2, 0 °C to rt; (b) BBr_3 (17% in CH_2Cl_2), CH_2Cl_2, 0 °C to rt; (c) 6-aminobenzothiazole-2-thiol, K_2CO_3, acetone, reflux; (d) $POCl_3$, DMF, ethyl acetate, rt; (e) Bromoalkane, K_2CO_3, KI, DMF, 80 °C; (f) CH_3I, K_2CO_3, DMF, 40 °C; (g) $NaClO_2$, $NaH_2PO_4{\cdot}2H_2O$, t-BuOH, rt; (h) $SOCl_2$, CH_2Cl_2, DMF, 0 °C to rt; (i) K_2CO_3, CH_2Cl_2, rt.

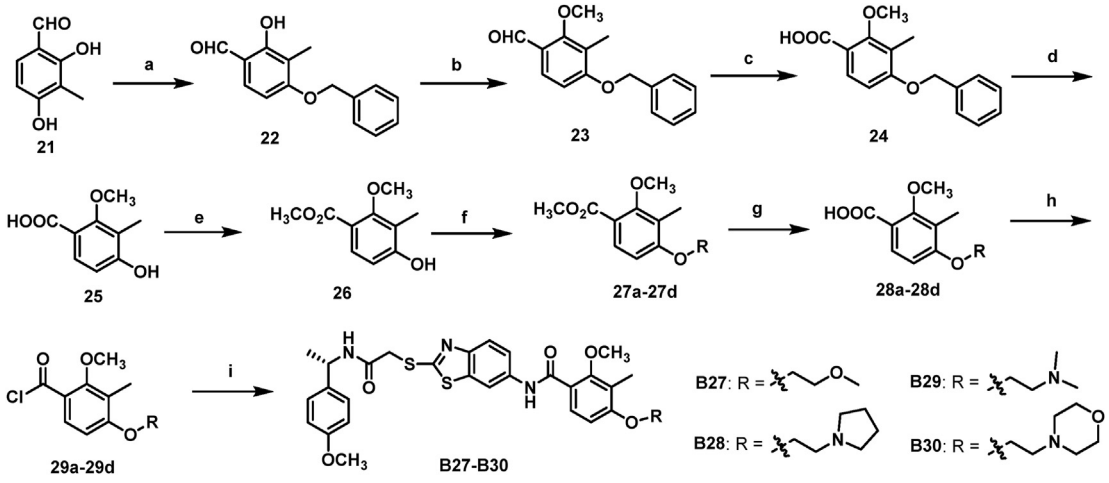

Scheme 4. Synthesis of compounds **B27**–**B30**. Reagents and conditions: (a) Benzyl bromide, KI, K_2CO_3, acetonitrile, 80 °C; (b) CH_3I, K_2CO_3, DMF, 40 °C; (c)$NaClO_2$, $NaH_2PO_4{\cdot}2H_2O$, t-BuOH, rt; (d) Pd/C, H_2, rt; (e) SO_2Cl_2, CH_3OH, rt; (f) Cs_2CO_3, anhydrous DMF, 85 °C and 1-bromo-2-methoxyethane for **27a**, 1-(2-chloroethyl)pyrrolidine hydrochloride and KI for **27b,** 2-chloro-N,N-dimethylethan-1-amine hydrochloride and KI for **27c**, 4-(2-chloroethyl)morpholine hydrochloride and KI for **27d**; (g) 1 M NaOH (aq.), CH_3OH, 50 °C, **28a**; 6 M HCl (aq.), 85 °C, **28b**-**28d**; (h) $SOCl_2$, CH_2Cl_2, DMF, rt; (i) **14a**, K_2CO_3, CH_2Cl_2, rt.

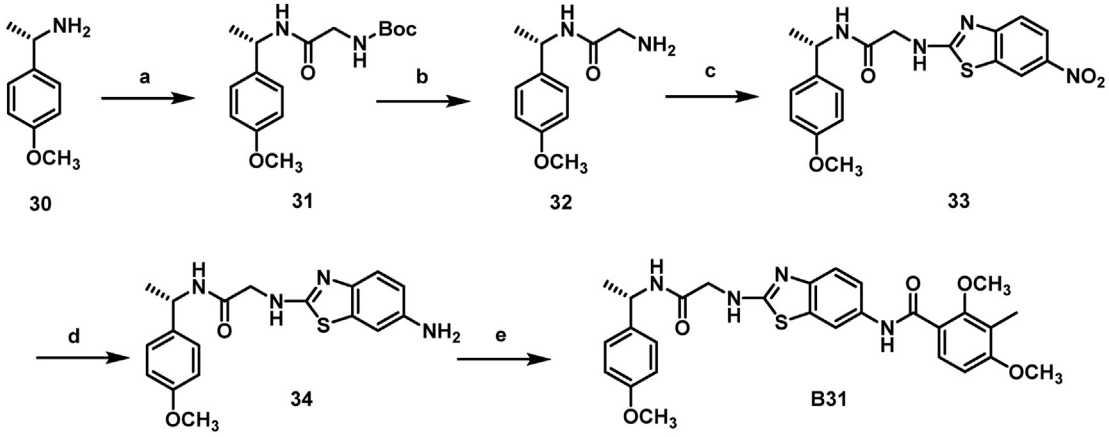

Scheme 5. Synthesis of compound **B31**. Reagents and conditions: (a) (*tert*-butoxycarbonyl)glycine, HATU, HoAt, DIPEA, THF, rt; (b) CF_3COOH, CH_2Cl_2, 0 °C; (c) 2-chloro-6-nitrobenzo[*d*]thiazole, n-Butanol, Et_3N, reflux; (d) Fe powder, NH_4Cl, $EtOH/H_2O$, reflux; (e) **20d**, K_2CO_3, CH_2Cl_2, rt.

The synthetic route of compound **B31** was shown in Scheme 5. Intermediate **31** was prepared by coupling commercially available compound **30** with N-Boc-glycine using HATU and DIPEA in 92.8% yield. Then, removing the Boc group and coupling with 2-chloro-6-nitrobenzo*[d]*thiazole to get compound **33**, which was converted to **B31** by reduction of the nitro group and condensation with **20d** sequentially.

Compound **B32** was synthesized as depicted in Scheme 6. Commercially available 2-chloro-6-aminobenzothiazole was converted to intermediate **36** followed by nucleophilic substitution reaction with ethyl glycolate to obtain **37** in 64.6% yield. After hydrolysis of the ethyl ester group of **37** and then condensation with intermediate **30,** the target compound **B32** was afforded.

2.3. Biological assays

2.3.1. Inhibitory activity on STAT3 transcription

Compounds **B1**–**B18** were firstly subjected to test the IL6/STAT3 signaling pathway activities using a STAT3 luciferase reporter system and their IC_{50} values were summarized in Table 1 (compounds **LLL12** [26] and **16w** were used as positive controls). For the substituent groups at R^1 position, compound **B1** with a methyl group showed better inhibitory activity (IC_{50} = 0.95 μM) than hit compound **16w** (IC_{50} = 1.60 μM). Incorporation of big steric substituents, such as ethyl (**B7**) and n-propyl (**B8**), in this position was detrimental to the activity (IC_{50} > 10 μM). Also, the presence of electron-withdrawing groups such as fluorine (**B3**), cyano (**B6**) and trifluoromethyl (**B9**) decreased the activity (IC_{50} > 10 μM). Compounds **B2** and **B5** with methoxyl and bromine at this position displayed similar activities to **16w** with IC_{50} values of 1.42 μM and 2.15 μM, respectively. For the substituent groups at R^2 position, there exists a similar trend as R^1 group. Substituent groups methyl (**B10**), methoxy (**B11**) and chlorine (**B13**) maintained the activities, while electron withdrawing group fluorine (**B12**) led to a significant loss of potency. Since there was a chiral methyl group at the long alkyl chain, we then investigated its effect on the activity. As shown in Table 2, the *R* configuration showed a better luciferase activity than *S* configuration (**B15** vs **B16**). Furthermore, the introduction of a methyl (**B17**) or a methoxyl group (**B18**) at R^2 position resulted in a 2-fold or 6-fold increased activity respectively (**B17**, IC_{50} = 0.46 μM; **B18** IC_{50} = 0.16 μM). Presumably the formation of an intramolecular hydrogen bond between OCH_3 and the adjacent NH of amide in compound **B18** made the amide and the benzene ring in the same plane ，and thus restricted the degrees of freedom. For this reason, **B18** was probably maintained in a preferred conformation. Therefore, the methyl at R^1 position could fit into the desired pocket more appropriately and increased the binding affinity with the target [41].

To further improve the potency of **B18**, it was envisioned that an additional hydrogen-bond or some hydrophobic interaction could be formed after introducing a hydroxy or methoxy at some positions of aromatic ring B. As shown in Table 3, compound **B19** with a methoxyl group at the para position exhibited the most potent activity with an IC_{50} value of 0.067 μM, which was better than a hydroxy substituted at the same position (**B21**, IC_{50} = 0.20 μM) and a methoxyl group at the meta position (**B20,** IC_{50} = 0.27 μM). However, activities of compounds with a hydroxy substituent at the ortho (**B23**, IC_{50} = 0.17 μM) or meta (**B22**, IC_{50} = 0.15 μM) position were comparable to that of compound **B18**. With the goals of improving solubility or simplify the molecule, we sought to shorten the long alkyl chain or replaced it with hydrophilic functional groups (**B24**–**B30**). As shown in Table 3, compared with **B18**, all resulting compounds showed reduced activities with IC_{50} values ranging from 0.20 μM to 1.03 μM, which might be due to the hydrophobic interactions between the alkyl chain and the target. Unfortunately, replacing the S atom of thioether with NH (**B31**) or O (**B32**) brought a significant drop of activities.

2.3.2. In vitro cell growth inhibitory activity

Compounds that displayed better inhibitory activity on STAT3 transcription were firstly evaluated for their antiproliferative activities against human erythroleukemia (HEL) cells bearing *JAK2* V617F mutation that results in constitutive activation of STAT3. JAK1/2 inhibitors **INC18424** and **AZD1480** were used as positive controls. As shown in Table 4, compared to the hit compound **16w**, all of these selected compounds exhibited potent activities toward HEL (*JAK2* V617F) cells except for **B1** and **B28**. Additionally, those compounds were tested their antiproliferative activities against STAT3 over-expressed human breast cancer cell line MDA-MB-468 using MTT assay. The IC_{50} values were listed in Table 4 and all the compounds showed growth inhibitory effect on the MDA-MB-468 cells with IC_{50} values ranging from sub-micromole to micromole (0.25 μM–6.57 μM). In particular, compound **B19** exhibiting the best STAT3-induced luciferase activity (IC_{50} = 0.067 μM) also displayed the most potent activity against MDA-MB-468 cells (IC_{50} = 0.25 μM). In contrast, **B18** and **B19** showed no antiproliferative activities against MDA-MB-453 and MCF-7 cell lines, which were generally reported with low expression levels of STAT3 [42], with IC_{50} values greater than 20 μM (Table 5). These data together suggested that a subset of compounds with potent antiproliferative activity were worth further evaluation.

2.3.3. Western blot analysis

Based on the results of inhibitory activities on STAT3 transcription and cell proliferation, we next proceeded to evaluate the inhibitory effect of compounds **B18** and **B19** on STAT3 signaling pathway in HEL (*JAK2* V617F) and MDA-MB-468 cells by Western blot analysis. STAT3 phosphorylation at Tyr705 residue can lead to

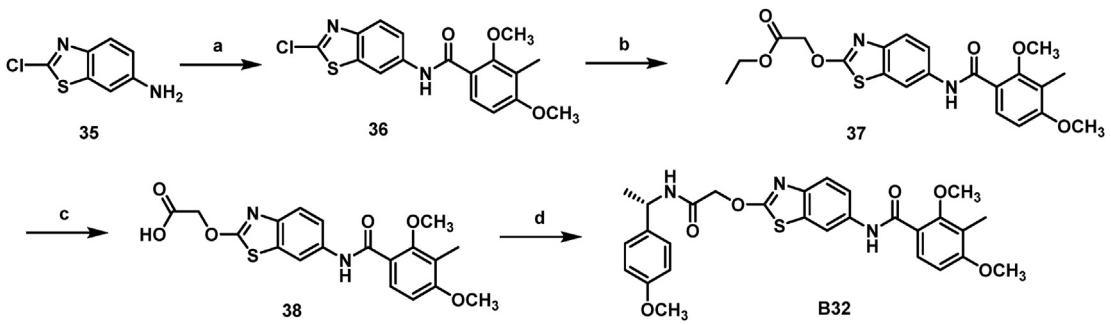

Scheme 6. Synthesis of compound **39**. Reagents and conditions: (a) **20d**, K_2CO_3, CH_2Cl_2, r. t.; (b) Ethyl-2-hydroxyacetate, NaH, THF, 70 °C; (c) 1 M NaOH (aq.), CH_3OH/THF, rt; (d) **11b**, HATU, HoAt, DIPEA, THF, rt.

Table 1
Inhibitory activity on STAT3 transcription as indicated by luciferase reporter gene assay.

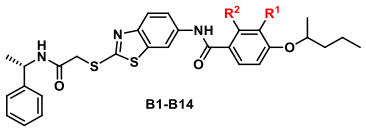

B1-B14

Compd.	R^1	R^2	IL-6/STAT3 pathway[a] IC_{50}±SD (μM)[b]	Compd.	R^1	R^2	IL-6/STAT3 pathway[a] IC_{50}±SD (μM)[b]
B1	CH_3	H	0.95 ± 0.22	**B9**	CF_3	H	>10
B2	OCH_3	H	1.42 ± 0.37	**B10**	H	CH_3	2.72 ± 0.72
B3	F	H	>10	**B11**	H	OCH_3	2.20 ± 0.27
B4	Cl	H	>10	**B12**	H	F	>10
B5	Br	H	2.15 ± 0.61	**B13**	H	Cl	1.34 ± 0.21
B6	CN	H	>10	**B14**	F	F	>10
B7	C_2H_5	H	>10	**16w**	H	H	1.60 ± 0.12
B8	$CH_2CH_2CH_3$	H	>10	**LLL12**			0.098 ± 0.01

[a] STAT3-dependent luciferase reporter gene assay in HepG2 cell.
[b] The data are the mean ± SD from at least three independent experiments.

Table 2
Inhibitory activity on STAT3 transcription as indicated by luciferase reporter gene assay.

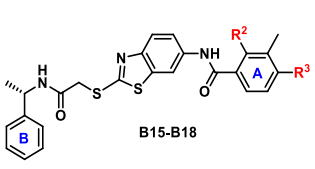

B15-B18

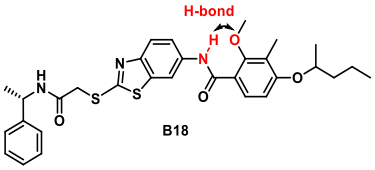

B18

Compd.	R^2	R^3	IL-6/STAT3 pathway[a] IC_{50}±SD (μM)[b]
B1	H		0.95 ± 0.22
B15	H		0.90 ± 0.13
B16	H		1.20 ± 0.05
B17	CH_3		0.46 ± 0.01
B18	OCH_3		0.16 ± 0.03
LLL12			0.098 ± 0.01

[a] STAT3-dependent luciferase reporter gene assay in HepG2 cell.
[b] The data are the mean ± SD from at least three independent experiments.

its homodimerization, translocation into nucleus, DNA-binding and downstream transcriptional activities. There is an increasing understanding about phosphorylation at Ser727 residue, which is associated with the transcription, mitochondrial import and other biological functions of STAT3 [43]. Therefore, the STAT3 phosphorylation level at Tyr705 and Ser727 was evaluated. As shown in Fig. 3, these two compounds could inhibit STAT3 phosphorylation at Tyr705 and Ser727 in both cell lines without influence on the total expression of STAT3 protein after 24 h incubation. Aberrant STAT3 signaling has been shown to promote tumor progression through directly or indirectly upregulating the expression of downstream target genes, such as cell-cycle regulator *c-MYC* and an anti-apoptotic gene *MCL-1* [44,45]. Compounds **B18** and **B19** significantly reduced the protein level of c-Myc and MCL-1. Overall,

Table 3
Inhibitory activity on STAT3 transcription as indicated by luciferase reporter gene assay.

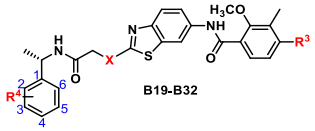

B19-B32

Compd.	R^3	R^4	X	IL-6/STAT3 pathway[a] IC_{50}±SD (μM)[b]
B18		H	S	0.16 ± 0.03
B19		4-OCH_3	S	0.067 ± 0.00
B20		3-OCH_3	S	0.27 ± 0.00
B21		4-OH	S	0.20 ± 0.11
B22		3-OH	S	0.15 ± 0.01
B23		2-OH	S	0.17 ± 0.01
B24		4-OCH_3	S	0.20 ± 0.02
B25		4-OCH_3	S	0.22 ± 0.00
B26	OCH_3	4-OCH_3	S	0.12 ± 0.03
B27		4-OCH_3	S	0.26 ± 0.10
B28		4-OCH_3	S	1.03 ± 0.10
B29		4-OCH_3	S	0.52 ± 0.07
B30		4-OCH_3	S	0.24 ± 0.01
B31	OCH_3	4-OCH_3	NH	1.49 ± 0.15
B32	OCH_3	4-OCH_3	O	8.86 ± 0.16
LLL12				0.098 ± 0.01

[a] STAT3-dependent luciferase reporter gene assay in HepG2 cell.
[b] The data are the mean ± SD from at least three independent experiments.

Table 4
Antiproliferative activity of the representative compounds against HEL (*JAK2* V617F) and MDA-MB-468 cells.

Compd.	HEL (*JAK2* V617F)[a] IC_{50}±SD (μM)[b]	MDA-MB-468[a] IC_{50}±SD (μM)[b]
16w	>10	2.21 ± 0.20
B1	>10	0.73 ± 0.02
B17	0.93 ± 0.16	0.81 ± 0.16
B18	2.41 ± 0.73	1.04 ± 0.27
B19	1.11 ± 0.17	0.25 ± 0.05
B20	0.87 ± 0.19	0.50 ± 0.04
B21	0.68 ± 0.25	0.70 ± 0.03
B22	0.62 ± 0.20	2.24 ± 0.18
B23	0.97 ± 0.22	0.59 ± 0.19
B24	2.05 ± 1.05	2.02 ± 0.15
B25	1.29 ± 0.08	1.81 ± 0.09
B26	1.34 ± 0.06	2.05 ± 0.23
B27	1.44 ± 0.03	1.16 ± 0.16
B28	10.4 ± 1.41	3.36 ± 0.32
B29	4.98 ± 0.61	6.57 ± 0.64
B30	3.38 ± 1.22	1.77 ± 0.55
LLL12	1.46 ± 0.33	0.73 ± 0.03
Stattic	1.59 ± 0.35	1.92 ± 0.08
INCB18424	1.40 ± 0.20	>20
AZD1480	0.73 ± 0.07	5.87 ± 0.87

[a] The inhibitory effects of these compounds on the proliferation of cancer cell lines were determined by the MTT assay.
[b] The data are the mean ± SD from at least three independent experiments.

Table 5
Antiproliferative activity of **B18** and **B19** against MDA-MB-453 and MCF-7 cells.

Compd.	MDA-MB-453[a]	MCF-7[a]
	IC_{50}±SD (μM)[b]	IC_{50}±SD (μM)[b]
B18	>20	>20
B19	>20	>20
Stattic	4.40 ± 0.16	1.70 ± 0.10

[a] The inhibitory effects of these compounds on the proliferation of cancer cell lines were determined by the MTT assay.
[b] The data are the mean ± SD from at least two independent experiments.

the results indicated these compounds efficiently inhibited STAT3 signaling pathway.

2.3.4. *In vitro kinases activity test*

To further evaluate the selectivity of compounds **B18** and **B19** against the upstream kinases which could activate STAT3 signaling pathway, enzyme-linked immunosorbent assay (ELISA) was employed to test a panel of kinases. As shown in Table 6, we investigated the inhibitory effects of compounds **B18** and **B19** on eleven receptor tyrosine kinases. Encouragingly, all of our compounds had no effect against these kinases, which clearly manifested that the inhibition of p-STAT3 was not owing to the inhibition of upstream kinases.

2.3.5. *The selectivity against related IFN-γ/STAT1 and TNF-α/NF-κB signaling pathways*

To our knowledge, IFN-γ/STAT1 and TNF-α/NF-κB signaling pathways are two closely related intracellular signaling pathways with IL-6/STAT3 signaling pathway. The former is the structural homologous signaling pathway, and the latter is the functional homologous signaling pathway. Therefore, the selectivity of compounds **B18** and **B19** against these two signaling pathway was investigated using a STAT1 luciferase reporter gene assay in HepG2 cells and a NF-κB luciferase reporter gene assay in HEK-293 cells. As shown in Table 7, compounds **B18** and **B19** did not display any of TNF-α-induced NF-κB activations with a concentration as high as 100 μM. However, both compounds showed little selectivity for STAT3 signaling over IFN-γ/STAT1 signaling pathway, probably owing to the high structural homology of the SH2 domain among the STAT proteins. Thus, improving STAT isoform selectivity remains a goal for future compound optimization.

2.3.6. *Apoptosis induction and G2/M cell-cycle arrest in MDA-MB-468 and HEL cells*

As compounds **B18** and **B19** displayed potent antiproliferative potency toward both MDA-MB-468 and HEL (*JAK2* V617F) cell lines, we then investigated the effect of them on the induction of cells apoptosis by flow cytometry. As shown in Fig. 4A, compounds **B18** and **B19** induced apoptosis of the test cells at the concentrations of 1.25 μM, 2.5 μM and 5.0 μM, which demonstrated that **B18** and **B19** could effectively inhibit cancer cell growth through apoptosis induction. Also, the effect of **B18** and **B19** on cell cycle progression of MDA-MB-468 and HEL (*JAK2* V617F) cells was determined using flow cytometry and the results were shown in Fig. 4B. After treatment with compounds **B18** and **B19** for 48 h, the proportion of cells in G2/M phase was increased accompanying with a decrease of cells in G1 phase in a dose-dependent behavior.

2.3.7. *SPR assay*

To determine the binding affinity and kinetic parameters of our representative compounds toward STAT3 SH2 domain, surface plasmon resonance (SPR) assay was employed using a Biacore T200 optical biosensor. Firstly, the reported STAT3 SH2 domain binders 5-FAM-GpYLPQTV-NH2 derived peptide (**Sub**) [46] and **Stattic** [47]

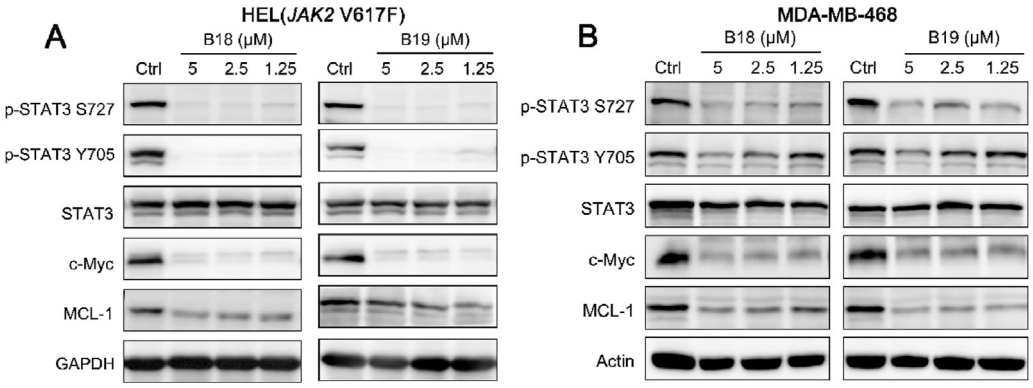

Fig. 3. Western blot analysis of the inhibition of STAT3 phosphorylation at Tyr705 and Ser727, the downstream target proteins (c-Myc, MCL-1) by compounds **B18** and **B19** in (A) HEL (*JAK2* V617F) and (B) MDA-MB-468 cells.

Table 6
Inhibitory activities against a panel of representative kinases.

Compd.	Inhibition rate at 1.0 μM (%)[a]										
	JAK1	JAK2	JAK3	VEGFR-1	PDGFR-β	EGFR	ErbB2	ErbB4	Abl	Eph-A2	IGF1R
B18	−2.2	−0.6	−4.7	0.0	0.0	0.0	5.2	0.0	4.7	1.1	0.0
B19	3.3	4.0	−6.8	0.0	0.0	0.0	9.6	0.0	4.1	0.0	0.0
INCB018424	80.4	91.7	78.5	/	/	/	/	/	/	/	/
Su11248	/	/	/	86.4	76.1	/	/	/	/	/	/
BIBW2992	/	/	/	/	/	98.9	93.4	88.6	/	/	/
Dasatinib	/	/	/	/	/	/	/	/	100	100	/
AEW541	/	/	/	/	/	/	/	/	/	/	100

[a] The inhibition rates are the mean of three independent experiments.

Table 7
Inhibitory activity against related IFN-γ/STAT1 and TNF-α/NF-κB signaling pathways.

Compd.	IL-6/STAT3[a] IC_{50}±SD (μM)[d]	IFN-γ/STAT1[b] IC_{50}±SD (μM)[d]	TNF-α/NF-κB[c] IC_{50}±SD (μM)[d]
B18	0.16 ± 0.03	0.35 ± 0.01	>100
B19	0.067 ± 0.00	0.32 ± 0.02	>100
BBI608	0.84 ± 0.07	0.88 ± 0.08	3.55 ± 0.21

[a] STAT3-dependent luciferase reporter gene assay in HepG2 cell.
[b] STAT1-dependent luciferase reporter gene assay in HepG2 cell.
[c] NF-κB -dependent luciferase reporter gene assay in HEK-293 cell.
[d] The data are the mean ± SD from at least three independent experiments.

were used as positive controls. As shown in Fig. 5, the equilibrium constant K_D values of compounds **Sub** and **Stattic** were 28.81 nM and 1528 nM respectively. For our representative compounds **B18** and **B19**, the response unit (RU) values were proportional to compound concentrations within the selected ranges and the K_D values were 62.61 nM (**B18**) and 53.04 nM (**B19**) respectively, which indicated a strong binding affinity to STAT3 SH2 domain.

2.3.8. Fluorescence polarization (FP) assay

It has been reported that the binding site of 5-FAM-GpYLPQTV-NH_2 derived peptide (**Sub**) and **Sttatic** was pTyr705 site in SH2 domain of STAT3 [46,47]. To exclude the directly binding at pTyr705 site of our compounds **B18** and **B19**, FP-based competition binding assay was conducted according to previously reported method [47,48]. Firstly, this derived peptide was applied as the fluorescent probe with the K_D value of 186.4 nM in our experiment, which was almost equivalent to the reported value (K_D = 150 nM) by Berg and coworker [46]. As shown in Table 8, **Stattic** could bind to STAT3 protein in a concentration-dependent manner, indicating its binding position at pTyr705 site in SH2 domain. However, compounds **B18** and **B19** did not show any competition with the probe even at a concentration of 100 μM, which indicates their binding site was different from **Stattic** and the probe (**Sub**).

2.3.9. Molecular docking study

As **B19** exhibited the most potent inhibitory activity in luciferase reporter assay among all designed compounds, a docking model of **B19** bound to SH2 domain was generated on the basis of the crystal structure of the STAT3β homodimer (PDB code 1BG1) by Schrodinger, Maestro suite. As illustrated in Fig. 6B, **B19** located at the Leu706-Phe 710 (Phe710-lys709-thr708-lys707-leu706) binding site in STAT3 SH2 domain rather than the pY705 site and acted as a partial peptidomimetic of phosphotyrosine peptide (pYLKTKF). The left amide NH and the right amide C═O formed two hydrogen bonds with Gln644 and Glu638 respectively. In addition, the oxygen atom close to the long alkyl chain formed one hydrogen bond with the amide group of Gln635 (Fig. 6C). The 4-methoxy-*S*-methyl

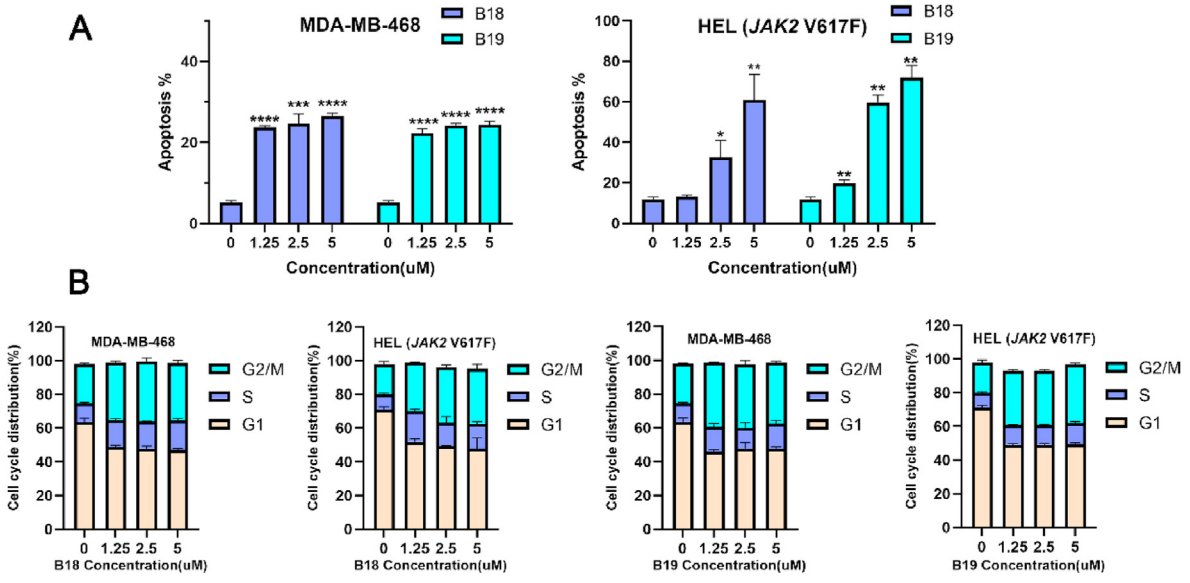

Fig. 4. Induction of apoptosis and cell-cycle arrest by compounds **B18** and **B19** in MDA-MB-468 and HEL cells. (A) Effects of compounds **B18** and **B19** on the induction of apoptosis. The cells were treated with increasing concentrations of the test compounds for 48 h and analyzed by annexin V/propidium iodide double staining. The data are representative of three independent experiments. ****, $p < 0.0001$, ***, $p < 0.001$, **, $p < 0.01$, *, $p < 0.05$. (B) Cell cycle analysis of compound **B18** and **B19** by flow cytometry. The cells were treated with increasing concentrations of test compounds for 48 h.

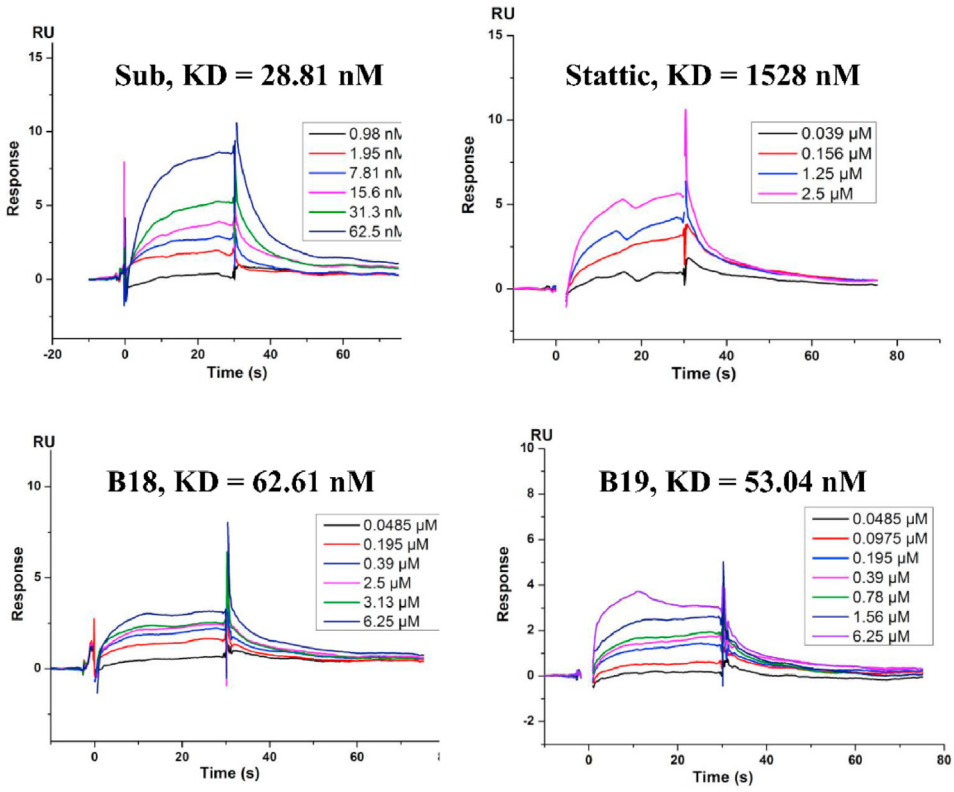

Fig. 5. SPR analysis of representative compounds with STAT3 SH2 domain. For **Sub**, compound concentrations were varied from 0.98 to 62.5 nM; for **Stattic**, compound concentrations were varied from 0.039 to 2.5 μM; For compound **B18** and **B19**, a concentration range of 0.0485−6.25 μM was used. Time was measured in seconds.

Table 8
FP-based competition binding assay of **B18, B19** and **Stattic.**

Compds.	Binding rate (%)		
	100 μM	50 μM	20 μM
B18	<10	<10	<10
B19	<10	<10	<10
Stattic	95.0	71.1	62.3

[a] The binding rates are the mean of three independent experiments.

benzylamine group occupied the hydrophobic pocket surrounded by Met648、Tyr640、Ile653、Ile711 residues (S2) in a manner similar to Phe710 of the phosphotyrosine peptide. The methyl on the right benzene ring fitted perfectly the expectant hydrophobic cleft described before and enhanced the binding affinity via hydrophobic interactions with Phe716, Ile659 and Trp623. Intriguingly, the O atom of the methoxyl adjacent to this methyl group could form an intramolecular hydrogen bond with the NH of amide, which was conductive to the insertion of methyl into the described hydrophobic cleft and made a great improvement on activity (Fig. 6D).

3. Conclusions

In this work, we reported a series of potent STAT3 inhibitors by optimizing the previously identified benzothiazole derivatives. Among the tested compounds, we found that compound **B19** exhibited the most potent activities against STAT3 transcription and inhibited cancer cell growth, such as MDA-MB-468 and HEL (*JAK2* V617F) cells, at low micromole concentration. Further biochemical study demonstrated that **B19** could dose-dependently inhibited STAT3 phosphorylation at Tyr705 and Ser727, as well as the downstream gene expression (*c-MYC* and *MCL-1*). In addition, compound **B19** was highly selective for the IL-6/STAT3 signaling pathway over TNF-α/NF-κB signaling pathway and some upstream kinases. Mechanistically, we elucidated the predicted binding mode of **B19** at the Leu706-Phe 710 binding site of STAT3 SH2 domain using SPR, FP and molecular docking studies. All of those results indicated that targeting the Leu706-Phe710 binding site in STAT3 SH2 could prevent either STAT3 recruitment to the receptor and phosphorylation at Tyr705 by JAKs, or the formation of STAT3 dimerization, subsequently inhibiting the translocation of STAT3 dimers to nucleus to induce transcription of downstream genes. However, **B19** exhibited poor oral exposures with low area under the concentration time curve (AUC_{last}) values (3 mg/kg, 2.50 h ng/mL) which may be caused by the poor solubility, the oxidative metabolism of S atom, the hydrolysis of two amide bond or the cleavage of carbon-sulfur bond. Accordingly, several structural optimizations to improve metabolism stability should be conducted in the future work, including bioisosteric replacement of the amide bond, incorporation of methyl, fluoro, *gem*-dimethyl or *gem*-difluoro at the methylene position to improve the oxidative metabolism, and introduction of heteroatoms to reduce the lipophilicity.

4. Experimental section

4.1. Chemistry

All the reagents and solvents were purchased from Adamas-beta®, Energy Chemical or Bide pharmatech and were used without further purification unless otherwise noted. Anhydrous solvents were purchased from Adamas-beta®. ^{1}H NMR and ^{13}C NMR spectra were recorded on a 400 MHz Varian spectrometer or a

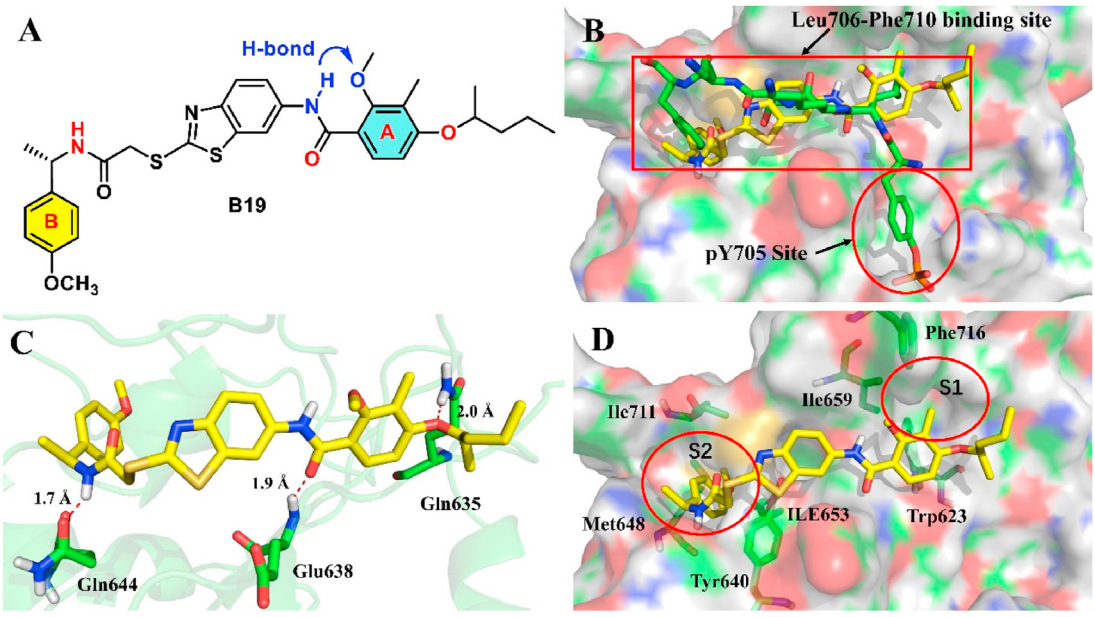

Fig. 6. Molecular docking study of **B19** in STAT3 SH2 domain (PDB code: 1BG1). (A) Chemical structure of compound **B19**. (B) Superimposed pose of **B19** (yellow) and pY705-Phe 710 peptide (green) bound in the surface of binding site. (C) Predicted hydrogen bonds interaction of **B19** (yellow) within STAT3 SH2 domain. (D) **B19** (yellow) bound in the surface of binding site. The figures were generated using Pymol.

600 MHz Bruker spectrometer at 303 K and referenced to TMS. ^{19}F NMR spectrum was recorded on a 600 MHz Bruker spectrometer at 303 K. Chemical shifts are reported in parts per million (ppm, δ). Proton coupling patterns are described as follows: s, singlet; d, doublet; t, triplet; q, quartet; dd, doublet of doublets; dt, doublet of triplets; brs, broad singlet. Mass spectra data were obtained on Agilent Technologies 1260 infinity LC/MS instrument (ESI-MS) and High-resolution mass spectra (HRMS) data were given by AB 5600 + Q TOF. Analytical and preparative TLCs were performed on silica gel HSGF/UV 254. The chromatograms were conducted on silica gel (200–300 mesh) and visualized under UV light at 254 and 365 nm.

*4.1.1. General procedures for the synthesis of **B1**–**B14***

The synthesis of the products **B1**–**B14** from 4-hydrobenzoic acid derivatives and (*S*) methyl benzylamine was previously reported in ref. 32.

*4.1.1.1. 3-Methyl-N-(2-((2-oxo-2-(((S)-1-phenylethyl)amino)ethyl) thio)Benzo[d]thiazol-6-yl)-4-(pentan-2-yloxy)benzamide (**B1**).* The title compound was obtained starting from **3** (0.20 mmol, 68.7 mg) and 3-methyl-4-(pentan-2-yloxy)benzoyl chloride (**6a**, 0.24 mmol, 57.8 mg). The residue was purified by flash column chromatography on silica gel (200–300 mesh) using petroleum ether/ethyl acetate eluent (PE/EA = 3/1, v/v) to afford the desired product as white solid (90.2 mg, 82.5% yield). ^{1}H NMR (400 MHz, DMSO-d_6) δ 10.24 (s, 1H), 8.78 (d, J = 7.82 Hz, 1H), 8.47 (d, J = 1.57 Hz, 1H), 7.80–7.70 (m, 4H), 7.31–7.24 (m, 4H), 7.19 (t, J = 7.04 Hz, 1H), 7.06 (d, J = 8.22 Hz, 1H), 4.95–4.85 (m, 1H), 4.60–4.52 (m, 1H), 4.17 (d, J = 14.9 Hz, 1H), 4.12 (d, J = 14.9 Hz, 1H), 2.18 (s, 3H), 1.70–1.62 (m, 1H), 1.60–1.52 (m, 1H), 1.48–1.33 (m, 5H), 1.25 (d, J = 5.87 Hz, 3H), 0.89 (t, J = 7.43 Hz, 3H). ^{13}C NMR (100 MHz, DMSO-d_6) δ 165.13, 164.92, 164.02, 158.32, 148.32, 143.77, 135.86, 134.81, 129.78, 127.84, 126.88, 126.31, 125.88, 125.52, 125.43, 120.40, 119.36, 112.06, 111.28, 72.71, 48.11, 37.63, 36.27, 22.05, 19.18, 17.70, 15.86, 13.56. ESI-HRMS $[M+H]^+$ calcd for $C_{30}H_{34}N_3O_3S_2$: 548.2036, found: 548.2039.

*4.1.1.2. 3-Methoxy-N-(2-((2-oxo-2-(((S)-1-phenylethyl)amino)ethyl) thio)benzo[d] thiazol-6-yl)-4-(pentan-2-yloxy)benzamide (**B2**).* The title compound was obtained starting from **3** (0.20 mmol, 68.7 mg) and 3-methoxy-4-(pentan-2-yloxy)benzoyl chloride (**6b**, 0.24 mmol, 61.6 mg). The residue was purified by flash column chromatography on silica gel (200–300 mesh) using petroleum ether/ethyl acetate eluent (PE/EA = 3/1, v/v) to afford the desired product as white solid (73.1 mg, 64.9% yield). ^{1}H NMR (400 MHz, DMSO-d_6) δ 10.25 (s, 1H), 8.76 (d, J = 7.9 Hz, 1H), 8.44 (d, J = 1.5 Hz, 1H), 7.76 (d, J = 8.8 Hz, 1H), 7.71 (dd, J = 8.9, 1.7 Hz, 1H), 7.56 (dd, J = 8.4, 1.6 Hz, 1H), 7.51 (d, J = 1.7 Hz, 1H), 7.33–7.22 (m, 4H), 7.17 (t, J = 6.9 Hz, 1H), 7.07 (d, J = 8.5 Hz, 1H), 4.94–4.84 (m, 1H), 4.56–4.46 (m, 1H), 4.16 (d, J = 14.9 Hz, 1H), 4.12 (d, J = 14.9 Hz, 1H), 3.81 (s, 3H), 1.69–1.59 (m, 1H), 1.56–1.46 (m, 1H), 1.43–1.29 (m, 5H), 1.21 (d, J = 6.0 Hz, 3H), 0.87 (t, J = 7.3 Hz, 3H). ^{13}C NMR (100 MHz, DMSO-d_6) δ 165.60, 165.20, 164.62, 150.22, 149.24, 148.91, 144.26, 136.20, 135.29, 128.33, 126.79, 126.70, 126.02, 121.16, 120.89, 120.04, 113.57, 112.82, 111.61, 73.76, 55.74, 48.58, 38.04, 36.77, 22.54, 19.59, 18.22, 14.00. ESI-HRMS $[M+H]^+$ calcd for $C_{30}H_{34}N_3O_4S_2$: 564.1985, found: 564.1983.

*4.1.1.3. 3-Fluoro-N-(2-((2-oxo-2-(((S)-1-phenylethyl)amino)ethyl) thio)benzo[d] thiazol-6-yl)-4-(pentan-2-yloxy)benzamide (**B3**).* The title compound was obtained starting from **3** (0.20 mmol, 68.7 mg) and 3-fluoro-4-(pentan-2-yloxy)benzoyl chloride (**6c**, 0.24 mmol, 58.7 mg). The residue was purified by flash column chromatography on silica gel (200–300 mesh) using petroleum ether/ethyl acetate eluent (PE/EA = 3/1, v/v) to afford the desired product as white solid (91.2 mg, 82.7% yield). ^{1}H NMR (400 MHz, DMSO-d_6) δ 10.34 (s, 1H), 8.79 (d, J = 7.8 Hz, 1H), 8.48 (s, 1H), 7.87–7.69 (m, 4H), 7.36–7.15 (m, 6H), 4.95–4.85 (m, 1H), 4.68–4.58 (m, 1H), 4.18 (d, J = 15.0 Hz, 1H), 4.12 (d, J = 15.0 Hz, 1H), 1.72–1.61 (m, 1H), 1.59–1.50 (m, 1H), 1.47–1.34 (m, 5H), 1.27 (d, J = 6.0 Hz, 3H), 0.89 (t, J = 7.3 Hz, 3H). ^{13}C NMR (100 MHz, DMSO-d_6) δ 165.93, 165.14, 164.39, 153.31, 150.89, 149.41, 149.01, 144.64, 136.40, 135.71, 128.69, 127.16, 126.41, 125.37, 121.31, 120.31, 116.17, 116.01, 113.14, 75.28, 48.95, 38.27, 37.20, 22.88, 19.89, 18.49, 14.32.^{19}F NMR

(565 MHz, $CDCl_3$) δ −131.83. ESI-HRMS $[M+H]^+$ calcd for $C_{29}H_{31}FN_3O_3S_2$: 552.1785, found: 552.1781.

*4.1.1.4. 3-Chloro-N-(2-((2-oxo-2-(((S)-1-phenylethyl)amino)ethyl) thio)benzo[d]thiazol-6-yl)-4-(pentan-2-yloxy)benzamide (**B4**).* The title compound was obtained starting from **3** (0.20 mmol, 68.7 mg) and 3-chloro-4-(pentan-2-yloxy)benzoyl chloride (**6d**, 0.24 mmol, 62.7 mg). The residue was purified by flash column chromatography on silica gel (200−300 mesh) using petroleum ether/ethyl acetate eluent (PE/EA = 3/1, v/v) to afford the desired product as white solid (68.8 mg, 60.7% yield). ^{1}H NMR (400 MHz, DMSO-d_6) δ 10.38 (s, 1H), 8.79 (d, J = 7.7 Hz, 1H), 8.47 (s, 1H), 8.06 (s, 1H), 7.92 (d, J = 8.6 Hz, 1H), 7.81−7.68 (m, 2H), 7.36−7.16 (m, 5H), 4.95−4.85 (m, 1H), 4.71−4.61 (m, 1H), 4.23−4.09 (m, 2H), 1.74−1.63 (m, 1H), 1.63−1.54 (m, 1H), 1.51−1.39 (m, 2H), 1.36 (d, J = 7.0 Hz, 3H), 1.28 (d, J = 6.0 Hz, 3H), 0.89 (t, J = 7.3 Hz, 3H). ^{13}C NMR (100 MHz, DMSO-d_6) δ 165.45, 164.68, 163.81, 155.84, 148.89, 144.15, 135.87, 135.19, 129.44, 128.37, 128.20, 127.13, 126.66, 125.90, 121.85, 120.80, 119.80, 114.22, 112.66, 74.74, 48.45, 37.75, 36.65, 22.41, 19.36, 17.94, 13.84. ESI-HRMS $[M + H]^+$ calcd for $C_{29}H_{31}ClN_3O_3S_2$: 568.1490, found: 568.1487.

*4.1.1.5. 3-Bromo-N-(2-((2-oxo-2-(((S)-1-phenylethyl)amino)ethyl) thio)benzo[d]thiazol -6-yl)-4-(pentan-2-yloxy)benzamide (**B5**).* The title compound was obtained starting from **3** (0.20 mmol, 68.7 mg) and 3-bromo-4-(pentan-2-yloxy)benzoyl chloride (**6e**, 0.24 mmol, 73.3 mg). The residue was purified by flash column chromatography on silica gel (200−300 mesh) using petroleum ether/ethyl acetate eluent (PE/EA = 3/1, v/v) to afford the desired product as white solid (74.3 mg, 60.6% yield). ^{1}H NMR (400 MHz, DMSO-d_6) δ 10.38 (s, 1H), 8.79 (d, J = 7.9 Hz, 1H), 8.46 (d, J = 1.7 Hz, 1H), 8.21 (d, J = 2.1 Hz, 1H), 7.96 (dd, J = 8.7, 2.0 Hz, 1H), 7.80−7.67 (m, 2H), 7.40−7.10 (m, 6H), 4.95−4.85 (m, 1H), 4.70−4.61 (m, 1H), 4.17 (d, J = 14.9 Hz, 1H), 4.12 (d, J = 14.9 Hz, 1H), 1.73−1.63 (m, 1H), 1.62−1.53 (m, 1H), 1.50−1.33 (m, 5H), 1.28 (d, J = 6.0 Hz, 3H), 0.88 (t, J = 7.3 Hz, 3H). ^{13}C NMR (100 MHz, DMSO-d_6) δ 165.65, 164.84, 163.89, 156.89, 149.04, 144.29, 136.01, 135.34, 132.60, 129.20, 128.36, 127.69, 126.83, 126.04, 120.96, 119.98, 114.13, 112.84, 111.72, 74.97, 48.64, 37.94, 36.79, 22.56, 19.52, 18.10, 14.02. ESI-HRMS $[M+H]^+$ calcd for $C_{29}H_{31}BrN_3O_3S_2$: 614.0967, found: 614.0963.

*4.1.1.6. 3-Cyano-N-(2-((2-oxo-2-(((S)-1-phenylethyl)amino)ethyl) thio)benzo[d]thiazol -6-yl)-4-(pentan-2-yloxy)benzamide (**B6**).* The title compound was obtained starting from **3** (0.20 mmol, 68.7 mg) and 3-cyano-4-(pentan-2-yloxy)benzoyl chloride (**6f**, 0.24 mmol, 60.4 mg). The residue was purified by flash column chromatography on silica gel (200−300 mesh) using petroleum ether/ethyl acetate eluent (PE/EA = 3/1, v/v) to afford the desired product as white solid (96.2 mg, 86.2% yield). ^{1}H NMR (400 MHz, DMSO-d_6) δ 10.46 (s, 1H), 8.80 (d, J = 7.9 Hz, 1H), 8.51 (d, J = 2.0 Hz, 1H), 8.39 (d, J = 2.3 Hz, 1H), 8.24 (dd, J = 9.0, 2.3 Hz, 1H), 7.82 (d, J = 8.8 Hz, 1H), 7.74 (dd, J = 8.9, 2.0 Hz, 1H), 7.46 (d, J = 9.2 Hz, 1H), 7.36−7.27 (m, 4H), 7.25−7.19 (m, 1H), 4.98−4.88 (m, 1H), 4.84−4.74 (m, 1H), 4.21 (d, J = 14.9 Hz, 1H), 4.17 (d, J = 14.9 Hz, 1H), 1.78−1.68 (m, 1H), 1.67−1.58 (m, 1H), 1.51−1.36 (m, 5H), 1.34 (d, J = 6.0 Hz, 3H), 0.93 (t, J = 7.4 Hz, 3H). ^{13}C NMR (150 MHz, DMSO-d_6) δ 165.31, 164.66, 163.14, 161.71, 148.87, 144.00, 135.61, 135.11, 134.67, 133.26, 128.06, 126.73, 126.53, 125.78, 120.73, 119.63, 115.79, 113.64, 112.52, 100.88, 75.29, 48.33, 37.45, 36.57, 22.23, 19.09, 17.72, 13.66. ESI-HRMS $[M+H]^+$ calcd for $C_{30}H_{31}N_4O_3S_2$: 559.1832, found: 559.1833.

*4.1.1.7. 3-Ethyl-N-(2-((2-oxo-2-(((S)-1-phenylethyl)amino)ethyl) thio)benzo[d]thiazol -6-yl)-4-(pentan-2-yloxy)benzamide (**B7**).* The title compound was obtained starting from **3** (0.20 mmol, 68.7 mg) and 3-ethyl-4-(pentan-2-yloxy)benzoyl chloride (**6g**, 0.24 mmol, 61.2 mg). The residue was purified by flash column chromatography on silica gel (200−300 mesh) using petroleum ether/ethyl acetate eluent (PE/EA = 3/1, v/v) to afford the desired product as white solid (56.7 mg, 50.5% yield). ^{1}H NMR (400 MHz, DMSO-d_6) δ 10.24 (s, 1H), 8.79 (d, J = 7.9 Hz, 1H), 8.47 (d, J = 1.7 Hz, 1H), 7.83−7.70 (m, 4H), 7.33−7.23 (m, 4H), 7.19 (t, J = 7.0 Hz, 1H), 7.07 (d, J = 8.8 Hz, 1H), 4.95−4.85 (m, 1H), 4.64−4.54 (m, 1H), 4.18 (d, J = 14.8, 1H), 4.13 (d, J = 14.8, 1H), 2.59 (q, J = 7.5 Hz, 2H), 1.72−1.62 (m, 1H), 1.61−1.51 (m, 1H), 1.50−1.34 (m, 5H), 1.24 (d, J = 6.0 Hz, 3H), 1.15 (t, J = 7.5 Hz, 3H), 0.89 (t, J = 7.3 Hz, 3H). ^{13}C NMR (100 MHz, DMSO-d_6) δ 165.46, 165.29, 164.38, 158.20, 148.71, 144.15, 136.23, 135.17, 132.11, 128.73, 128.20, 127.22, 126.66, 125.90, 120.75, 119.78, 112.51, 111.63, 72.66, 48.45, 38.00, 36.65, 23.09, 22.40, 19.39, 18.07, 14.11, 13.91. ESI-HRMS $[M+H]^+$ calcd for $C_{31}H_{36}N_3O_3S_2$: 562.2193, found: 562.2193.

*4.1.1.8. N-(2-((2-oxo-2-(((S)-1-phenylethyl)amino)ethyl)thio)benzo [d]thiazol-6-yl)-4-(pentan-2-yloxy)-3-propylbenzamide (**B8**).* The title compound was obtained starting from **3** (0.20 mmol, 68.7 mg) and 4-(pentan-2-yloxy)-3-propylbenzoyl chloride (**6h**, 0.24 mmol, 64.5 mg). The residue was purified by flash column chromatography on silica gel (200−300 mesh) using petroleum ether/ethyl acetate eluent (PE/EA = 3/1, v/v) to afford the desired product as white solid (50.0 mg, 43.5% yield). ^{1}H NMR (400 MHz, DMSO-d_6) δ 10.23 (s, 1H), 8.79 (d, J = 7.9 Hz, 1H), 8.47 (d, J = 1.8 Hz, 1H), 7.83−7.70 (m, 4H), 7.33−7.23 (m, 4H), 7.19 (t, J = 7.0 Hz, 1H), 7.07 (d, J = 8.9 Hz, 1H), 4.95−4.85 (m, 1H), 4.63−4.54 (m, 1H), 4.18 (d, J = 14.9, 1H), 4.13 (d, J = 14.9, 1H), 2.55 (t, J = 7.6 Hz, 2H), 1.73−1.38 (m, 6H), 1.36 (d, J = 7.0 Hz, 3H), 1.24 (d, J = 6.0 Hz, 3H), 0.89 (t, J = 7.3 Hz, 6H). ^{13}C NMR (100 MHz, DMSO-d_6) δ 165.45, 165.25, 164.36, 158.32, 148.72, 144.14, 136.25, 135.17, 130.54, 129.53, 128.20, 127.26, 126.66, 125.91, 125.77, 120.75, 119.79, 112.52, 111.67, 72.62, 48.45, 38.00, 36.69, 31.88, 22.49, 22.39, 19.34, 18.02, 13.92, 13.88. ESI-HRMS $[M+H]^+$ calcd for $C_{32}H_{38}N_3O_3S_2$: 576.2349, found: 576.2350.

*4.1.1.9. N-(2-((2-oxo-2-(((S)-1-phenylethyl)amino)ethyl)thio)benzo [d]thiazol-6-yl)-4- (pentan-2-yloxy)-3-(trifluoromethyl)benzamide (**B9**).* The title compound was obtained starting from **3** (0.20 mmol, 68.7 mg) and 4-(pentan-2-yloxy)-3-(trifluoromethyl) benzoyl chloride (**6i**, 0.24 mmol, 70.7 mg). The residue was purified by flash column chromatography on silica gel (200−300 mesh) using petroleum ether/ethyl acetate eluent (PE/EA = 3/1, v/v) to afford the desired product as white solid (56.3 mg, 46.8% yield). ^{1}H NMR (400 MHz, $CDCl_3$) δ 8.40 (d, J = 1.8 Hz, 1H), 8.24 (s, 1H), 8.13−8.06 (m, 2H), 7.87 (d, J = 7.7 Hz, 1H), 7.65 (d, J = 8.7 Hz, 1H), 7.44 (dd, J = 8.7, 2.0 Hz, 1H), 7.24−7.17 (m, 4H), 7.07 (d, J = 8.7 Hz, 1H), 5.11−5.01 (m, 1H), 4.64−4.54 (m, 1H), 3.96 (d, J = 14.9 Hz, 1H), 3.91 (d, J = 14.9 Hz, 1H), 1.86−1.76 (m, 1H), 1.70−1.60 (m, 2H), 1.56−1.47 (m, 1H), 1.44 (d, J = 6.9 Hz, 3H), 1.37 (d, J = 6.1 Hz, 3H), 0.96 (t, J = 7.3 Hz, 3H). ^{13}C NMR (100 MHz, DMSO-d_6) δ 165.93, 165.23, 164.36, 158.81, 149.48, 144.64, 136.33, 135.71, 134.40, 128.69, 127.16, 126.41, 126.35, 121.31, 120.41, 114.59, 113.32, 74.96, 48.95, 38.25, 37.20, 22.88, 19.61, 18.24, 14.28.^{19}F NMR (565 MHz, $CDCl_3$) δ −62.68. ESI-HRMS $[M+H]^+$ calcd for $C_{30}H_{31}F_3N_3O_3S_2$: 602.1753, found: 602.1751.

*4.1.1.10. 2-Methyl-N-(2-((2-oxo-2-(((S)-1-phenylethyl)amino)ethyl) thio)benzo[d] thiazol-6-yl)-4-(pentan-2-yloxy)benzamide (**B10**).* The title compound was obtained starting from **3** (0.20 mmol, 68.7 mg) and 2-methyl-4-(pentan-2-yloxy)benzoyl chloride (**6j**, 0.24 mmol, 57.8 mg). The residue was purified by flash column chromatography on silica gel (200−300 mesh) using petroleum ether/ethyl acetate eluent (PE/EA = 3/1, v/v) to afford the desired product as white solid (44.5 mg, 40.7% yield). ^{1}H NMR (400 MHz,

DMSO-d_6) δ 10.36 (s, 1H), 8.79 (d, J = 7.9 Hz, 1H), 8.48 (d, J = 1.6 Hz, 1H), 7.75 (d, J = 8.8 Hz, 1H), 7.64 (dd, J = 8.9, 1.8 Hz, 1H), 7.42 (d, J = 9.1 Hz, 1H), 7.35–7.15 (m, 5H), 6.81 (d, J = 6.8 Hz, 2H), 4.94–4.84 (m, 1H), 4.54–4.46 (m, 1H), 4.16 (d, J = 14.9 Hz, 1H), 4.11 (d, J = 14.9 Hz, 1H), 2.36 (s, 3H), 1.67–1.58 (m, 1H), 1.56–1.48 (m, 1H), 1.46–1.32 (m, 5H), 1.21 (d, J = 6.0 Hz, 3H), 0.87 (t, J = 7.3 Hz, 3H). ^{13}C NMR (100 MHz, DMSO-d_6) δ 167.93, 165.78, 164.42, 159.08, 148.88, 144.35, 138.34, 136.52, 135.51, 129.58, 128.96, 128.45, 126.93, 126.12, 121.11, 119.30, 117.83, 112.20, 111.93, 72.89, 48.72, 38.13, 36.81, 22.62, 20.00, 19.71, 18.34, 14.10. ESI-HRMS $[M+H]^+$ calcd for $C_{30}H_{34}N_3O_3S_2$: 548.2036, found: 548.2034.

*4.1.1.11. 2-Methoxy-N-(2-((2-oxo-2-(((S)-1-phenylethyl)amino) ethyl)thio)benzo[d] thiazol-6-yl)-4-(pentan-2-yloxy)benzamide (**B11**).* The title compound was obtained starting from **3** (0.20 mmol, 68.7 mg) and 2-methoxy-4-(pentan-2-yloxy)benzoyl chloride (**6k**, 0.24 mmol, 61.6 mg). The residue was purified by flash column chromatography on silica gel (200–300 mesh) using petroleum ether/ethyl acetate eluent (PE/EA = 3/1, v/v) to afford the desired product as white solid (45.6 mg, 40.5% yield). ^{1}H NMR (400 MHz, $CDCl_3$) δ 9.91 (s, 1H), 8.55 (d, J = 2.0 Hz, 1H), 8.24 (d, J = 8.8 Hz, 1H), 7.97 (d, J = 7.7 Hz, 1H), 7.66 (d, J = 8.7 Hz, 1H), 7.38 (dd, J = 8.7, 2.1 Hz, 1H), 7.25–7.16 (m, 5H), 6.64 (dd, J = 8.9, 2.2 Hz, 1H), 6.53 (d, J = 2.1 Hz, 1H), 5.11–5.02 (m, 1H), 4.54–4.44 (m, 1H), 4.05 (s, 3H), 3.96 (d, J = 14.9 Hz, 1H), 3.89 (d, J = 14.9 Hz, 1H), 1.79–1.75 (m, 1H), 1.63–1.57 (m, 1H), 1.54–1.41 (m, 5H), 1.34 (d, J = 6.1 Hz, 3H), 0.96 (t, J = 7.3 Hz, 3H). ^{13}C NMR (100 MHz, $CDCl_3$) δ 167.39, 165.08, 163.32, 162.78, 158.66, 148.60, 142.88, 136.53, 135.86, 134.16, 128.57, 127.22, 125.92, 121.05, 119.37, 113.71, 112.43, 106.96, 100.21, 73.95, 56.23, 49.39, 38.45, 36.32, 22.00, 19.66, 18.71, 14.02. ESI-HRMS $[M+H]^+$ calcd for $C_{30}H_{34}N_3O_4S_2$: 564.1985, found: 564.1989.

*4.1.1.12. 2-Fluoro-N-(2-((2-oxo-2-(((S)-1-phenylethyl)amino)ethyl) thio)benzo[d] thiazol -6-yl)-4-(pentan-2-yloxy)benzamide (**B12**).* The title compound was obtained starting from **3** (0.20 mmol, 68.7 mg) and 2-fluoro-4-(pentan-2-yloxy)benzoyl chloride (**6l**, 0.24 mmol, 58.7 mg). The residue was purified by flash column chromatography on silica gel (200–300 mesh) using petroleum ether/ethyl acetate eluent (PE/EA = 3/1, v/v) to afford the desired product as white solid (52.7 mg, 47.8% yield). ^{1}H NMR (400 MHz, DMSO-d_6) δ 10.39 (s, 1H), 8.79 (d, J = 7.9 Hz, 1H), 8.46 (d, J = 1.9 Hz, 1H), 7.76 (d, J = 8.8 Hz, 1H), 7.66–7.58 (m, 2H), 7.34–7.23 (m, 4H),7.22–7.16 (m, 1H), 6.94 (dd, J = 12.7, 2.0 Hz, 1H), 6.87 (dd, J = 8.6, 2.1 Hz, 1H), 4.95–4.84 (m, 1H), 4.63–4.53 (m, 1H), 4.18 (d, J = 14.9 Hz, 1H), 4.13 (d, J = 14.9 Hz, 1H), 1.67–1.58 (m, 1H), 1.57–1.49 (m, 1H), 1.46–1.30 (m, 5H), 1.24 (d, J = 6.0 Hz, 3H), 0.88 (t, J = 7.3 Hz, 3H). ^{13}C NMR (100 MHz, DMSO-d_6) δ 165.96, 165.15, 163.08, 162.12, 161.72, 159.64, 149.37, 144.63, 136.33, 135.82, 131.70, 128.70, 127.17, 126.40, 121.42, 119.71, 116.72, 112.34, 103.46, 74.17, 48.96, 38.22, 37.17, 22.87, 19.80, 18.52, 14.32.^{19}F NMR (565 MHz, $CDCl_3$) δ −110.46. ESI-HRMS $[M+H]^+$ calcd for $C_{29}H_{31}FN_3O_3S_2$: 552.1785, found: 552.1790.

*4.1.1.13. 2-Chloro-N-(2-((2-oxo-2-(((S)-1-phenylethyl)amino)ethyl) thio)benzo[d] thiazol-6-yl)-4-(pentan-2-yloxy)benzamide (**B13**).* The title compound was obtained starting from **3** (0.20 mmol, 68.7 mg) and 2-chloro-4-(pentan-2-yloxy)benzoyl chloride (**6m**, 0.24 mmol, 62.7 mg). The residue was purified by flash column chromatography on silica gel (200–300 mesh) using petroleum ether/ethyl acetate eluent (PE/EA = 3/1, v/v) to afford the desired product as white solid (59.5 mg, 52.5% yield). ^{1}H NMR (400 MHz, DMSO-d_6) δ 10.59 (s, 1H), 8.79 (d, J = 7.9 Hz, 1H), 8.47 (d, J = 1.5 Hz, 1H), 7.76 (d, J = 8.8 Hz, 1H), 7.62 (dd, J = 8.8, 1.7 Hz, 1H), 7.51 (d, J = 8.5 Hz, 1H), 7.32–7.22 (m, 4H), 7.19 (t, J = 6.9 Hz, 1H), 7.09 (d, J = 2.1 Hz, 1H), 6.99 (dd, J = 8.6, 2.2 Hz, 1H), 4.95–4.84 (m, 1H), 4.61–4.52 (m, 1H), 4.17 (d, J = 14.9 Hz, 1H), 4.12 (d, J = 15.0 Hz, 1H), 1.67–1.59 (m, 1H), 1.56–1.48 (m, 1H), 1.45–1.29 (m, 5H), 1.23 (d, J = 6.0 Hz, 3H), 0.88 (t, J = 7.3 Hz, 3H). ^{13}C NMR (100 MHz, DMSO-d_6) δ 170.70, 170.13, 169.91, 164.57, 154.05, 150.97, 149.32, 141.04, 140.56, 136.51, 135.57, 133.81, 133.41, 131.89, 131.09, 129.02, 126.19, 121.51, 119.34, 78.74, 53.68, 42.93, 41.80, 27.60, 24.50, 23.24, 19.04. ESI-HRMS $[M+Na]^+$ calcd for $C_{29}H_{30}ClN_3O_3S_2Na$: 590.1309, found: 590.1314.

*4.1.1.14. 2,3-Difluoro-N-(2-((2-oxo-2-(((S)-1-phenylethyl)amino) ethyl)thio)benzo[d] thiazol-6-yl)-4-(pentan-2-yloxy)benzamide (**B14**).* The title compound was obtained starting from **3** (0.20 mmol, 68.7 mg) and 2,3-difluoro-4-(pentan-2-yloxy)benzoyl chloride (**6n**, 0.24 mmol, 63.0 mg). The residue was purified by flash column chromatography on silica gel (200–300 mesh) using petroleum ether/ethyl acetate eluent (PE/EA = 3/1, v/v) to afford the desired product as white solid (93.7 mg, 82.3% yield). ^{1}H NMR (400 MHz, DMSO-d_6) δ 10.55 (s, 1H), 8.79 (d, J = 7.9 Hz, 1H), 8.45 (d, J = 1.8 Hz, 1H), 7.78 (d, J = 8.8 Hz, 1H), 7.63 (dd, J = 8.8, 1.7 Hz, 1H), 7.49–7.43 (m, 1H), 7.33–7.24 (m, 4H), 7.22–7.14 (m, 2H), 4.95–4.86 (m, 1H), 4.69–4.61 (m, 1H), 4.18 (d, J = 14.9 Hz, 1H), 4.13 (d, J = 14.9 Hz, 1H), 1.73–1.64 (m, 1H), 1.61–1.53 (m, 1H), 1.47–1.33 (m, 5H), 1.28 (d, J = 6.0 Hz, 3H), 0.89 (t, J = 7.3 Hz, 3H). ^{13}C NMR (100 MHz, DMSO-d_6) δ 165.92, 165.38, 162.07, 149.52, 144.64, 136.07, 135.86, 128.69, 127.16, 126.41, 124.85, 121.48, 119.70, 118.33, 118.22, 112.61, 111.57, 76.09, 48.95, 38.17, 37.19, 22.88, 19.88, 18.45, 14.29.^{19}F NMR (565 MHz, $CDCl_3$) δ −137.42 (d, J = 21.4 Hz), −157.76 (d, J = 21.4 Hz). ESI-HRMS $[M+H]^+$ calcd for $C_{29}H_{30}F_2N_3O_3S_2$: 570.1691, found: 570.1696.

*4.1.2. Synthesis of **B15***

*4.1.2.1. Methyl (R)-3-methyl-4-(pentan-2-yloxy)benzoate (**8a**).* DEAD (0.695 mL, 4.41 mmol) was added dropwise to a stirred solution of $P(Ph)_3$ (1.16 g, 4.41 mmol) in anhydrous THF at 0 °C. When the reaction mixture became colourless, methyl 4-hydroxy-3-methylbenzoate (489 mg, 2.94 mmol) was added at 0 °C and stirred for 10 min. Subsequently, (*S*)-pentan-2-ol (0.32 mL, 2.94 mmol) was added at 0 °C and stirred for another 10 min. After the reaction mixture was stirred at room temperature for about 20 h, the solvent was evaporated under reduced pressure. The residue was dissolved in ethyl acetate (100 mL) and was washed with distilled water (100 mL) for three times. The organic phases were combined, dried over Na_2SO_4, and evaporated under reduced pressure. The crude compound was purified by silica gel column chromatography (PE/EA = 10/1, v/v) to give **8a** (270 mg, 38.9% yield). ^{1}H NMR (400 MHz, DMSO-d_6) δ 7.75 (d, J = 8.6 Hz, 1H), 7.72 (s, 1H), 7.01 (d, J = 8.6 Hz, 1H), 4.59–4.48 (m, 1H), 3.77 (s, 3H), 2.12 (s, 3H), 1.72–1.59 (m, 1H), 1.57–1.49 (m, 1H), 1.45–1.30 (m, 2H), 1.22 (d, J = 6.0 Hz, 3H), 0.86 (t, J = 7.3 Hz, 3H). ESI-MS: calcd for $[M+H]^+$ m/z 237.1, found: 237.1.

*4.1.2.2. (R)-3-methyl-4-(pentan-2-yloxy)benzoic acid (**9a**).* To a solution of **8a** (160 mg, 0.677 mmol) in methanol (5 mL) was added 1 M NaOH (5 mL, 5.00 mmol). The resulting mixture was stirred at 50 °C for 12 h. Upon cooling the methanol was removed under vacuum, and the residue was acidified to pH = 2 or below with HCl (1 M). Then the solution was extracted with ethyl acetate (20 mL × 3) and the combined organic solvents were dried with sodium sulfate and concentrated *in vacuo*. The crude compound was purified by silica gel column chromatography (DCM/CH_3OH = 15/1, v/v) to give **9a** (130 mg, 86.4% yield). ^{1}H NMR (400 MHz, $CDCl_3$) δ 7.92 (dd, J = 8.6, 2.1 Hz, 1H), 7.89 (d, J = 2.1 Hz, 1H), 6.83 (d, J = 8.6 Hz, 1H), 4.53–4.43 (m, 1H), 2.22 (s, 3H), 1.82–1.72 (m, 1H), 1.64–1.56 (m, 1H), 1.52–1.38 (m, 2H), 1.32 (d, J = 6.1 Hz, 3H), 0.94 (t, J = 7.3 Hz, 3H). ESI-MS: calcd for $[M-H]^-$ m/z

221.1, found: 221.1.

*4.1.2.3. (R)-3-methyl-4-(pentan-2-yloxy)benzoyl chloride (**10a**).* Thionyl chloride (10 mL, 1378 mmol) was added to **9a** (111 mg, 0.50 mmol) and stirred for 3 h under reflux condition. After cooling to room temperature, the thionyl chloride was evaporated under reduced pressure to obtain a yellow oil (**10a**), which was used directly for the following synthesis.

*4.1.2.4. 3-Methyl-N-(2-((2-oxo-2-(((S)-1-phenylethyl)amino)ethyl) thio)benzo[d]thiazol-6-yl)-4-(((R)-pentan-2-yl)oxy)benzamide (**B15**).* Compound **B15** was prepared in a similar manner as described for compounds **B1**−**B14**, starting from **3** (68.7 mg, 0.20 mmol) and **10a** (57.8 mg, 0.24 mmol). The residue was purified by flash column chromatography on silica gel (200−300 mesh) using petroleum ether/ethyl acetate eluent (PE/EA = 3/1, v/v) to afford the desired product as white solid (40.2 mg, 36.7% yield). ^{1}H NMR (400 MHz, DMSO-d_6) δ 10.24 (s, 1H), 8.79 (d, J = 7.9 Hz, 1H), 8.48 (d, J = 1.8 Hz, 1H), 7.83−7.68 (m, 4H), 7.34−7.16 (m, 5H), 7.06 (d, J = 8.5 Hz, 1H), 4.95−4.86 (m, 1H), 4.61−4.52 (m, 1H), 4.18 (d, J = 14.9, 1H), 4.13 (d, J = 14.9, 1H), 2.18 (s, 3H), 1.71−1.63 (m, 1H), 1.60−1.52 (m, 1H), 1.49−1.31 (m, 5H), 1.25 (d, J = 6.0 Hz, 3H), 0.89 (t, J = 7.3 Hz, 3H). ^{13}C NMR (100 MHz, DMSO-d_6) δ 165.47, 165.25, 164.36, 158.68, 148.68, 144.13, 136.24, 135.17, 130.14, 128.19, 127.23, 126.66, 126.23, 125.89, 125.82, 120.76, 119.70, 112.41, 111.64, 73.06, 48.45, 37.98, 36.64, 22.39, 19.53, 18.05, 16.20, 13.90. ESI-HRMS $[M+H]^+$ calcd for $C_{30}H_{34}N_3O_3S_2$: 548.2036, found: 548.2041.

*4.1.3. Synthesis of **B16***

*4.1.3.1. Methyl (S)-3-methyl-4-(pentan-2-yloxy)benzoate (**8b**).* Compound **8b** was prepared in a similar manner as described for compound **8a**, starting from **7a** (489 mg, 2.94 mmol) and (R)-pentan-2-ol (0.32 mL, 2.94 mmol). The residue was purified by flash column chromatography on silica gel (200−300 mesh) using petroleum ether/ethyl acetate eluent (PE/EA = 10/1, v/v) to afford the desired product as colorless oil (444 mg, 64.0% yield). ^{1}H NMR (400 MHz, $CDCl_3$) δ 7.85 (d, J = 2.0 Hz, 1H), 7.82 (s, 1H), 6.80 (d, J = 8.5 Hz, 1H), 4.52−4.36 (m, 1H), 3.87 (s, 3H), 2.21 (s, 3H), 1.80−1.70 (m, 1H), 1.65−1.53 (m, 1H), 1.52−1.37 (m, 2H), 1.31 (d, J = 6.1 Hz, 3H), 0.93 (t, J = 7.3 Hz, 3H). ESI-MS: calcd for $[M+H]^+$ m/z 237.1, found: 237.1.

*4.1.3.2. (S)-3-methyl-4-(pentan-2-yloxy)benzoic acid (**9b**).* Compound **9b** was prepared in a similar manner as described for compound **9a**, starting from **8b** (472 mg, 2.00 mmol). The residue was purified by flash column chromatography on silica gel (200−300 mesh) using dichloromethane/methanol eluent (DCM/CH_3OH = 15/1, v/v) to afford the desired product as colorless oil (444 mg, 100.0% yield). ^{1}H NMR (400 MHz, $CDCl_3$) δ 8.02 (dd, J = 8.6, 2.1 Hz, 1H), 7.99 (d, J = 2.1 Hz, 1H), 6.93 (d, J = 8.6 Hz, 1H), 4.63−4.53 (m, 1H), 2.32 (s, 3H), 1.90−1.80 (m, 1H), 1.72−1.64 (m, 1H), 1.60−1.46 (m, 2H), 1.42 (d, J = 6.1 Hz, 3H), 0.93 (t, J = 7.3 Hz, 3H). ESI-MS: calcd for $[M-H]^-$ m/z 221.1, found: 221.1.

*4.1.3.3. (S)-3-methyl-4-(pentan-2-yloxy)benzoic acid (**10b**).* Compound **10b** was prepared in a similar manner as described for compound **10a**, starting from **9b** (111 mg, 0.50 mmol).

*4.1.3.4. 3-Methyl-N-(2-((2-oxo-2-(((S)-1-phenylethyl)amino)ethyl) thio)benzo[d]thiazol -6-yl)-4-(((R)-pentan-2-yl)oxy)benzamide (**B16**).* Compound **B16** was prepared in a similar manner as described for compounds **B1**−**B14**, starting from **3** (68.7 mg, 0.20 mmol) and **10b** (57.8 mg, 0.24 mmol). The residue was purified by flash column chromatography on silica gel (200−300 mesh) using petroleum ether/ethyl acetate eluent (PE/EA = 3/1, v/v) to afford the desired product as white solid (67.8 mg, 62.0% yield). ^{1}H NMR (400 MHz, DMSO-d_6) δ 10.25 (s, 1H), 8.80 (d, J = 8.0 Hz, 1H), 8.47 (d, J = 1.7 Hz, 1H), 7.84−7.66 (m, 4H), 7.33−7.16 (m, 5H), 7.05 (d, J = 8.5 Hz, 1H), 4.95−4.86 (m, 1H), 4.61−4.52 (m, 1H), 4.18 (d, J = 14.9, 1H), 4.13 (d, J = 14.9, 1H), 2.18 (s, 3H), 1.71−1.61 (m, 1H), 1.60−1.52 (m, 1H), 1.46−1.31 (m, 5H), 1.25 (d, J = 6.0 Hz, 3H), 0.88 (t, J = 7.3 Hz, 3H). ^{13}C NMR (100 MHz, DMSO-d_6) δ 165.49, 165.27, 164.38, 158.69, 148.69, 144.13, 136.23, 135.17, 130.14, 128.20, 127.24, 126.67, 126.24, 125.89, 125.80, 120.76, 119.72, 112.42, 111.64, 73.06, 48.46, 37.98, 36.63, 22.39, 19.53, 18.05, 16.21, 13.90. ESI-HRMS $[M+H]^+$ calcd for $C_{30}H_{34}N_3O_3S_2$: 548.2036, found: 548.2041.

*4.1.4. Synthesis of **B17***

*4.1.4.1. 2,3-Dimethyl-4-(pentan-2-yloxy)benzoic acid (**9c**).* Compound **8c** was synthesized following the synthetic procedure of compounds **5a-5n** and the crude product was obtained. Subsequently, NaOH (1 M) water solution (3 mL, 3.00 mmol) and CH_3OH (3 mL) were added and stirred for 1 h. Then the methanol was removed under vacuum, and the residue was acidified to pH = 2 or below with HCl (1 M). Then the solution was extracted with ethyl acetate (20 mL × 3) and the combined organic solvents were dried with sodium sulfate and concentrated *in vacuo*. The crude compound was purified by silica gel column chromatography (DCM/CH_3OH = 15/1, v/v) to give **9c** (white solid, two steps 51.0% yield). ^{1}H NMR (400 MHz, DMSO-d_6) δ 12.40 (s, 1H), 7.60 (d, J = 8.7 Hz, 1H), 6.83 (d, J = 8.8 Hz, 1H), 4.54−4.41 (m, 1H), 2.40 (s, 3H), 2.07 (s, 3H), 1.70−1.59 (m, 1H), 1.56−1.48 (m, 1H), 1.45−1.27 (m, 2H), 1.20 (d, J = 6.0 Hz, 3H), 0.86 (t, J = 7.3 Hz, 3H). ESI-MS: calcd for $[M-H]^-$ m/z 235.1, found: 235.1.

*4.1.4.2. 2,3-Dimethyl-4-(pentan-2-yloxy)benzoyl chloride (**10c**).* Compound **10c** was prepared in a similar manner as described for compound **10a**, starting from **9c** (118 mg, 0.50 mmol).

*4.1.4.3. 2,3-Dimethyl-N-(2-((2-oxo-2-(((S)-1-phenylethyl)amino) ethyl)thio)benzo[d] thiazol-6-yl)-4-(pentan-2-yloxy)benzamide (**B17**).* Compound **B17** was prepared in a similar manner as described for compounds **B1**−**B14**, starting from **3** (68.7 mg, 0.20 mmol) and **10c** (61.1 mg, 0.24 mmol). The residue was purified by flash column chromatography on silica gel (200−300 mesh) using petroleum ether/ethyl acetate eluent (PE/EA = 3/1, v/v) to afford the desired product as white solid (67.3 mg, 60.0% yield). ^{1}H NMR (400 MHz, DMSO-d_6) δ 10.40 (s, 1H), 8.79 (d, J = 7.6 Hz, 1H), 8.50 (s, 1H), 7.75 (d, J = 8.9 Hz, 1H), 7.64 (d, J = 8.1 Hz, 1H), 7.33−7.15 (m, 6H), 6.88 (d, J = 8.5 Hz, 1H), 4.95−4.85 (m, 1H), 4.55−4.45 (m, 1H), 4.18 (d, J = 14.9, 1H), 4.13 (d, J = 14.9, 1H), 2.25 (s, 3H), 2.10 (s, 3H), 1.70−1.61 (m, 1H), 1.60−1.51 (m, 1H), 1.46−1.33 (m, 5H), 1.22 (d, J = 5.6 Hz, 3H), 0.88 (t, J = 7.0 Hz, 3H). ^{13}C NMR (100 MHz, DMSO-d_6) δ 168.53, 165.45, 164.31, 156.41, 148.65, 144.15, 136.38, 135.40, 135.32, 130.07, 128.21, 126.68, 125.93, 125.64, 120.89, 118.93, 111.53, 109.80, 73.18, 48.45, 38.09, 36.69, 22.40, 19.63, 18.13, 16.66, 13.94, 11.78. ESI-HRMS $[M+H]^+$ calcd for $C_{31}H_{36}N_3O_3S_2$: 562.2193, found: 562.2190.

*4.1.5. General procedures for the synthesis of **B18**−**B26***

*4.1.5.1. 2, 4-dihydroxy-3-methylbenzaldehyde (**16**).* DMF (6.2 mL, 80.56 mmol) and $POCl_3$ (8.1 mL, 88.61 mmol) were mixed and added to a stirred solution of 2-methylbenzene-1,3-diol (**15**, 5.0 g, 0.806 mmol) in ethyl acetate (100 mL) at room temperature. Then water (5 mL) was added to the mixture and stirred for about 2 h. The reaction mixture was extracted with ethyl acetate (20 mL × 3). The combined organic phases were dried with sodium sulfate and concentrated *in vacuo*. The crude compound was purified by silica gel column chromatography (PE/EA = 5/1, v/v) to give **16** (white solid, 79.9% yield). ^{1}H NMR (400 MHz, DMSO-d_6) δ 11.56 (s, 1H),

10.74 (s, 1H), 9.65 (d, J = 3.0 Hz, 1H), 7.38 (dd, J = 8.4, 3.8 Hz, 1H), 6.51 (d, J = 8.5 Hz, 1H), 1.93 (s, 3H). ESI-MS: calcd for $[M-H]^-$ m/z 151.1, found: 151.1.

4.1.5.2. General procedures for the synthesis of compounds ***17a-17c***. To a stirred solution of **16** (152 mg, 1.0 mmol) in DMF (10 mL) were added bromoalkane (302 mg, 2.0 mmol, 2-bromopentane for **17a**; 274 mg, 2.0 mmol, 1-bromo-2-methyl-propan for **17b**; 246 mg, 2.0 mmol, 2-bromopropane for **17c**)、K_2CO_3 (553 mg, 4.0 mmol) and KI (16.6 mg, 0.1 mmol). The mixture was stirred at 80 °C for about 6 h. After cooling and filtration on Celite, the solvent was removed under reduced pressure to obtain an oily residue, which was purified by flash column chromatography on silica (PE/EA = 10/1, v/v) to give **17a-17c**.

*4.1.5.2.1. 2-Hydroxy-3-methyl-4-(pentan-2-yloxy) benzaldehyde (**17a**).* Reddish oil, 60.0% yield, ^{1}H NMR (400 MHz, DMSO-d_6) δ 11.40 (s, 1H), 9.76 (s, 1H), 7.56 (d, J = 8.7 Hz, 1H), 6.74 (d, J = 8.8 Hz, 1H), 4.65–4.56 (m, 1H), 1.95 (s, 3H), 1.70–1.59 (m, 1H), 1.58–1.48 (m, 1H), 1.47–1.27 (m, 2H), 1.23 (d, J = 6.0 Hz, 3H), 0.86 (t, J = 7.3 Hz, 3H). ESI-MS: calcd for $[M-H]^-$ m/z 221.1, found: 221.1.

*4.1.5.2.2. 2-Hydroxy-4-isobutoxy-3-methylbenzaldehyde (**17b**).* Colorless oil, 75.0% yield, ^{1}H NMR (400 MHz, DMSO-d_6) δ 11.37 (s, 1H), 9.79 (s, 1H), 7.59 (d, J = 8.6 Hz, 1H), 6.72 (d, J = 8.7 Hz, 1H), 3.86 (d, J = 6.4 Hz, 2H), 2.11–2.02 (m, 1H), 2.00 (s, 3H), 0.98 (d, J = 6.7 Hz, 6H). ESI-MS: calcd for $[M+H]^+$ m/z 209.1, found: 209.1.

*4.1.5.2.3. 4-Isopropoxy-2-methoxy-3-methylbenzaldehyde (**17c**).* Colorless oil, 60.4% yield, ^{1}H NMR (400 MHz, DMSO-d_6) δ 11.39 (s, 1H), 9.78 (s, 1H), 7.57 (d, J = 8.6 Hz, 1H), 6.76 (d, J = 8.8 Hz, 1H), 4.85–4.67 (m, 1H), 1.96 (s, 3H), 1.28 (d, J = 6.0 Hz, 6H). ESI-MS: calcd for $[M+H]^+$ m/z 195.1, found:195.1.

4.1.5.3. General procedures for the synthesis of compounds ***18a-18d***. To a solution of **16** or **17a-17c** (1.0 mmol) in DMF (5 mL) were added CH_3I (124 mL, 2.0 mmol for **18a-18c**, 248 mL, 4.0 mmol for **18d**) and K_2CO_3 (690 mg, 5.0 mmol). The mixture was stirred at 40 °C. for about 6 h. After cooling and filtration on Celite, the mixture was extracted with ethyl acetate (20 mL × 3) and the combined organic solvents were washed with water (20 mL). Then the organic phase was dried with sodium sulfate and concentrated *in vacuo*. The crude compounds were purified by silica gel column chromatography (PE/EA = 7/1, v/v) to give **18a-18d.**

*4.1.5.3.1. 2-Methoxy-3-methyl-4-(pentan-2-yloxy) benzaldehyde (**18a**).* Yellow oil, 97.2% yield, ^{1}H NMR (400 MHz, $CDCl_3$) δ 10.21 (s, 1H), 7.70 (d, J = 8.7 Hz, 1H), 6.71 (d, J = 8.7 Hz, 1H), 4.54–4.42 (m, 1H), 3.85 (s, 3H), 2.14 (s, 3H), 1.82–1.70 (m, 1H), 1.64–1.55 (m, 1H), 1.54–1.36 (m, 2H), 1.32 (d, J = 6.1 Hz, 3H), 0.94 (t, J = 7.3 Hz, 3H). ESI-MS: calcd for $[M+H]^+$ m/z 237.3, found: 237.2.

*4.1.5.3.2. 4-Isobutoxy-2-methoxy-3-methylbenzaldehyde (**18b**).* Colorless oil, 93.0% yield, ^{1}H NMR (400 MHz, $CDCl_3$) δ 10.21 (s, 1H), 7.71 (d, J = 8.7 Hz, 1H), 6.70 (d, J = 8.7 Hz, 1H), 3.85 (s, 3H), 3.79 (d, J = 6.4 Hz, 2H), 2.17 (s, 3H), 2.17–2.06 (m, 1H), 1.06 (s, 3H), 1.04 (s, 3H). ESI-MS: calcd for $[M+H]^+$ m/z 223.1, found: 223.1.

*4.1.5.3.3. 4-Isopropoxy-2-methoxy-3-methylbenzaldehyde (**18c**).* Colorless oil, yield 90.0%, ^{1}H NMR (400 MHz, DMSO-d_6) δ 10.08 (s, 1H), 7.60 (d, J = 8.7 Hz, 1H), 6.94 (d, J = 8.8 Hz, 1H), 4.78–4.65 (m, 1H), 3.78 (s, 3H), 2.04 (s, 3H), 1.28 (d, J = 6.0 Hz, 6H). ESI-MS: calcd for $[M+H]^+$ m/z 209.1, found: 209.1.

*4.1.5.3.4. 2,4-Dimethoxy-3-methylbenzaldehyde (**18d**).* White solid, 85.0% yield, ^{1}H NMR (400 MHz, DMSO-d_6) δ 10.05 (s, 1H), 7.60 (d, J = 8.7 Hz, 1H), 6.91 (d, J = 8.7 Hz, 1H), 3.83 (s, 3H), 3.75 (s, 3H), 2.03 (s, 3H). ESI-MS: calcd for $[M+H]^+$ m/z 181.1, found:181.1.

4.1.5.4. General procedures for the synthesis of compounds ***19a-19d***. To a solution of **18a-18d** (1.0 mmol) in t-BuOH (8 mL) and 2-methyl-2-butene (4 mL, 47.6 mmol) were added $NaClO_2$ (543 mg, 6.0 mmol) and $NaH_2PO_4 \cdot 2H_2O$ (468 mg, 3.0 mmol) buffer solution (pH = 4.5, 8 mL) at 0 °C. Then the mixture was stirred at room temperature for about 1 h. The solution was extracted with ethyl acetate (20 mL × 3) and the organic layer was dried with sodium sulfate and concentrated *in vacuo*. The crude compounds were purified by silica gel column chromatography (DCM/CH_3OH = 10/1, v/v) to give **19a-19d**.

*4.1.5.4.1. 2-Methoxy-3-methyl-4-(pentan-2-yloxy) benzoic acid (**19a**).* White solid, 63.1% yield, ^{1}H NMR (400 MHz, DMSO-d_6) δ 12.40 (s, 1H), 7.60 (d, J = 8.8 Hz, 1H), 6.78 (d, J = 8.9 Hz, 1H), 4.55–4.42 (m, 1H), 3.66 (s, 3H), 2.01 (s, 3H), 1.69–1.58 (m, 1H), 1.56–1.48 (m, 1H), 1.44–1.29 (m, 2H), 1.21 (d, J = 6.0 Hz, 3H), 0.86 (t, J = 7.3 Hz, 3H). ESI-MS: calcd for $[M-H]^-$ m/z 251.1, found: 251.1.

*4.1.5.4.2. 4-Isobutoxy-2-methoxy-3-methylbenzoic acid (**19b**).* White solid, 83.0% yield, ^{1}H NMR (400 MHz, DMSO-d_6) δ 12.39 (s, 1H), 7.59 (d, J = 8.7 Hz, 1H), 6.76 (d, J = 8.7 Hz, 1H), 3.76 (d, J = 6.2 Hz, 2H), 3.66 (s, 3H), 2.04 (s, 3H), 2.04–1.95 (m, 1H), 0.96 (d, J = 6.6 Hz, 6H). ESI-MS: calcd for $[M-H]^-$ m/z 237.1, found: 237.1.

*4.1.5.4.3. 4-Isopropoxy-2-methoxy-3-methylbenzoic acid (**19c**).* White solid, 80.0% yield, ^{1}H NMR (400 MHz, DMSO-d_6) δ 12.39 (s, 1H), 7.60 (d, J = 8.7 Hz, 1H), 6.81 (d, J = 8.8 Hz, 1H), 4.71–4.58 (m, 1H), 3.67 (s, 3H), 2.02 (s, 3H), 1.27 (d, J = 6.0 Hz, 6H). ESI-MS: calcd for $[M-H]^-$ m/z 223.1, found: 223.1.

*4.1.5.4.4. 2,4-Dimethoxy-3-methylbenzoic acid (**19d**).* White solid, 79.6% yield, ^{1}H NMR (400 MHz, DMSO-d_6) δ 12.41 (s, 1H), 7.62 (d, J = 8.9 Hz, 1H), 6.79 (d, J = 8.8 Hz, 1H), 3.80 (s, 3H), 3.66 (s, 3H), 2.02 (s, 3H). ESI-MS: calcd for $[M-H]^-$ m/z 195.1, found: 195.1.

4.1.5.5. General procedures for the synthesis of ***20a-20d***. To a solution of **19a-19d** (0.51 mmol) in 5 mL anhydrous CH_2Cl_2 were added $SOCl_2$ (607 mg, 5.1 mmol) and DMF (1 drop) at 0 °C. The mixture was stirred at room temperature for 15 min. Then the solution was concentrated *in vacuo* giving **20a-20d**, which were used directly for the following synthesis.

4.1.5.6. General procedures for the synthesis of ***12b-12d***. 2-Chloroacetyl chloride (169 mg, 1.5 mmol) was added dropwise to a mixture of (*S*)-1-(4-methoxyphenyl)ethan-1-amine derivatives (1.0 mmol) and potassium carbonate (414 mg, 3.0 mmol) in 5 mL of dioxane originally at 0 °C with stirring. Then the resulting mixture was warmed to ambient temperature (25 °C) and stirred for 6 h. After removal of dioxane solvents under reduced pressure, water was added and extracted with ethyl acetate (20 mL × 3). The organic layer was combined and dried with sodium sulfate. The solution was evaporated to give the crude product, which was purified by silica gel column chromatography (PE/EA = 15/1, v/v) to obtain **12b-12d**.

*4.1.5.6.1. (S)-2-chloro-N-(1-(4-methoxyphenyl)ethyl)acetamide (**12b**).* White solid, 27.5% yield, ^{1}H NMR (400 MHz, DMSO-d_6) δ 8.59 (d, J = 7.5 Hz, 1H), 7.24 (d, J = 7.6 Hz, 2H), 6.89 (d, J = 7.2 Hz, 2H), 4.92–4.82 (m, 1H), 4.06 (s, 2H), 3.73 (d, J = 1.2 Hz, 3H), 1.35 (d, J = 6.5 Hz, 3H). ESI-MS: calcd for $[M+H]^+$ m/z 228.1, 230.1, found: 228.1, 230.1.

*4.1.5.6.2. (S)-2-chloro-N-(1-(3-methoxyphenyl)ethyl)acetamide (**12c**).* White solid, 35.5% yield, ^{1}H NMR (400 MHz, DMSO-d_6) δ 8.61 (d, J = 7.9 Hz, 1H), 7.20 (t, J = 8.1 Hz, 1H), 6.85 (d, J = 7.2 Hz, 2H), 6.79–6.75 (m, 1H), 4.89–4.79 (m, 1H), 4.04 (s, 2H), 3.71 (s, 3H), 1.32 (d, J = 7.0 Hz, 3H). ESI-MS: calcd for $[M+H]^+$ m/z 228.1, 230.1, found: 228.1, 230.1.

*4.1.5.6.3. (S)-2-chloro-N-(1-(2-methoxyphenyl)ethyl)acetamide (**12d**).* White solid, 79.7% yield, ^{1}H NMR (400 MHz, DMSO-d_6) δ 8.55 (d, J = 7.8 Hz, 1H), 7.25–7.15 (m, 2H), 6.94 (d, J = 8.2 Hz, 1H), 6.88 (t, J = 7.4 Hz, 1H), 5.20–5.08 (m, 1H), 4.05 (s, 2H), 3.77 (s, 3H), 1.25 (d, J = 6.9 Hz, 3H). ESI-MS: calcd for $[M+H]^+$ m/z 228.1, 230.1, found:

228.1, 230.1.

*4.1.5.7. General procedures for the synthesis of **13b-13d**.* To a solution of **12b-12d** (1.0 mmol) in anhydrous dichloromethane (10 mL) was added boron tribromide (17% in CH_2Cl_2, 1.25 g, 5.0 mmol) at 0 °C. Water (10 mL) was added after the reaction was stirred for 3 h. Then the mixture was stirred for another 30 min before the extraction with dichloromethane (10 mL × 3). The organic layer was combined and dried with sodium sulfate. The solvent was evaporated to give the crude product, which was purified by silica gel column chromatography (PE/EA = 10/1, v/v) to give **13b-13d**.

*4.1.5.7.1. (S)-2-chloro-N-(1-(4-hydroxyphenyl)ethyl)acetamide (**13b**).* White solid, 85.0% yield, ^{1}H NMR (400 MHz, DMSO-d_6) δ 9.29 (s, 1H), 8.50 (d, J = 7.7 Hz, 1H), 7.09 (d, J = 8.3 Hz, 2H), 6.68 (d, J = 8.3 Hz, 2H), 4.80 (quint, 1H), 4.02 (s, 2H), 1.31 (d, J = 6.9 Hz, 3H). ESI-MS: calcd for $[M+H]^+$ m/z 214.1, 216.1, found:214.1, 216.1.

*4.1.5.7.2. (S)-2-chloro-N-(1-(3-hydroxyphenyl)ethyl)acetamide (**13c**).* White solid, 85.5% yield, ^{1}H NMR (400 MHz, DMSO-d_6) δ 9.34 (s, 1H), 8.57 (d, J = 7.9 Hz, 1H), 7.07 (t, J = 7.8 Hz, 1H), 6.72−6.65 (m, 2H), 6.59 (dd, J = 8.0, 1.5 Hz, 1H), 4.83−4.73 (m, 1H), 4.02 (s, 2H), 1.30 (d, J = 7.0 Hz, 3H). ESI-MS: calcd for $[M+H]^+$ m/z 214.1, 216.1, found:214.1, 216.1.

*4.1.5.7.3. (S)-2-chloro-N-(1-(2-hydroxyphenyl)ethyl)acetamide (**13d**).* White solid, 82.8% yield, ^{1}H NMR (400 MHz, DMSO-d_6) δ 9.55 (s, 1H), 8.50 (d, J = 8.1 Hz, 1H), 7.13 (d, J = 7.6 Hz, 1H), 7.04−6.98 (m, 1H), 6.77−6.69 (m, 2H), 5.14−5.06 (m, 1H), 4.05 (s, 2H), 1.27 (d, J = 6.9 Hz, 3H). ESI-MS: calcd for $[M+H]^+$ m/z 214.1, 216.1, found:214.1, 216.1.

*4.1.5.8. General procedures for the synthesis of **14a-14e**.* The syntheses of the compounds **14a-14e** starting from 6-aminobenzothiazole-2-thiol (91.1 mg, 0.50 mmol) and **12b-12c** or **13b-13d** (0.50 mmol) were previously reported in ref. 32 (syntheses of **13a-g**) and the obtained intermediates were directly used for the following step.

*4.1.5.9. General procedures for the synthesis of **B18**−**B26**.* The syntheses of the products **B18**−**B26** from **20a-20d** (0.24 mmol) and **3** (68.7 mg, 0.20 mmol) or **14a-14e** (0.20 mmol) were similar to the previously reported method published in ref. 32. The residues were purified by flash column chromatography on silica gel (200−300 mesh) using petroleum ether/ethyl acetate eluent (PE/EA = 3/1, v/v) to afford the desired products.

*4.1.5.9.1. 2-Methoxy-3-methyl-N-(2-((2-oxo-2-(((S)-1-phenylethyl)amino)ethyl)thio) benzo[d]thiazol-6-yl)-4-(pentan-2-yloxy)benzamide (**B18**).* White solid, 50.7% yield, ^{1}H NMR (400 MHz, DMSO-d_6) δ 10.30 (s, 1H), 8.79 (d, J = 7.9 Hz, 1H), 8.49 (s, 1H), 7.75 (d, J = 8.6 Hz, 1H), 7.66 (d, J = 8.7 Hz, 1H), 7.46 (d, J = 8.6 Hz, 1H), 7.33−7.16 (m, 5H), 6.87 (d, J = 8.7 Hz, 1H), 4.95−4.85 (m, 1H), 4.55−4.47 (m, 1H), 4.16 (d, J = 14.9, 1H), 4.12 (d, J = 14.9, 1H) 3.71 (s, 3H), 2.08 (s, 3H), 1.70−1.61 (m, 1H), 1.59−1.50 (m, 1H), 1.47−1.27 (m, 5H), 1.23 (d, J = 6.0 Hz, 3H), 0.88 (t, J = 7.3 Hz, 3H). ^{13}C NMR (100 MHz, DMSO-d_6) δ 165.52, 164.85, 164.45, 158.76, 156.74, 148.73, 144.10, 136.03, 135.33, 128.21, 127.79, 126.68, 125.88, 121.27, 120.92, 119.80, 119.16, 111.82, 108.25, 73.41, 61.48, 48.47, 37.99, 36.60, 22.37, 19.55, 18.07, 13.89, 8.99. ESI-HRMS $[M+H]^+$ calcd for $C_{31}H_{36}N_3O_4S_2$: 578.2142, found: 578.2144.

*4.1.5.9.2. 2-Methoxy-N-(2-((2-(((S)-1-(4-methoxyphenyl)ethyl) amino)-2-oxoethyl)thio) benzo [d]thiazol-6-yl)-3-methyl-4-(pentan-2-yloxy)benzamide (**B19**).* White solid, 30.0% yield, ^{1}H NMR (400 MHz, $CDCl_3$) δ 10.12 (s, 1H), 8.62 (s, 1H), 8.06 (d, J = 8.9 Hz, 1H), 7.85 (d, J = 6.2 Hz, 1H), 7.69 (d, J = 7.7 Hz, 1H), 7.42 (d, J = 8.1 Hz, 1H), 7.15 (d, J = 7.6 Hz, 2H), 6.82 (d, J = 8.7 Hz, 1H), 6.77 (d, J = 7.5 Hz, 2H), 5.04 (quint, 1H), 4.51 (sext, 1H), 3.92 (brd, J = 14.7, 2H), 3.90 (s, 3H), 3.77 (s, 3H), 2.23 (s, 3H), 1.85−1.72 (m, 1H), 1.58−1.48 (m, 1H), 1.48−1.32 (m, 2H),1.44 (d, J = 5.7 Hz, 3H), 1.36 (d, J = 3.0 Hz, 3H), 0.98 (t, J = 6.4 Hz, 3H). ^{13}C NMR (100 MHz, $CDCl_3$) δ 167.20, 165.02, 163.65, 160.72, 158.70, 157.44, 148.76, 136.64, 135.96, 135.05, 130.12, 127.14, 121.24, 120.58, 118.95, 117.66, 113.90, 112.13, 108.79, 74.11, 61.76, 55.25, 48.80, 38.60, 36.36, 21.82, 19.77, 18.71, 14.08, 9.25. ESI-HRMS $[M+H]^+$ calcd for $C_{32}H_{38}N_3O_5S_2$: 608.2247, found: 608.2243.

*4.1.5.9.3. 2-Methoxy-N-(2-((2-(((S)-1-(3-methoxyphenyl)ethyl) amino)-2-oxoethyl)thio) benzo[d]thiazol-6-yl)-3-methyl-4-(pentan-2-yloxy)benzamide (**B20**).* White solid, 20.0% yield, ^{1}H NMR (400 MHz, $CDCl_3$) δ 10.09 (s, 1H), 8.58 (s, 1H), 8.02 (t, J = 7.9 Hz, 2H), 7.70 (d, J = 8.7 Hz, 1H), 7.39 (d, J = 8.7 Hz, 1H), 7.15 (t, J = 7.9 Hz, 1H), 6.82−6.70 (m, 4H), 5.04 (quint, 1H), 4.51 (sext, 1H), 3.93 (s, 2H), 3.87 (s, 3H), 3.69 (s, 3H), 2.20 (s, 3H), 1.83−1.71 (m, 1H), 1.67−1.53 (m, 3H), 1.42 (d, J = 6.8 Hz, 3H), 1.33 (d, J = 6.0 Hz, 3H), 0.95 (t, J = 7.2 Hz, 3H). ^{13}C NMR (150 MHz, $CDCl_3$) δ 166.72, 164.58, 163.02, 160.10, 159.14, 156.82, 148.08, 144.03, 136.00, 135.38, 129.50, 129.01, 120.66, 119.95, 118.35, 117.56, 117.08, 111.91, 111.49, 111.20, 108.19, 73.50, 61.12, 54.48, 48.75, 37.98, 35.75, 21.39, 19.14, 18.07, 13.43, 8.60. ESI-HRMS $[M+H]^+$ calcd for $C_{32}H_{37}N_3O_5S_2$: 608.2247, found: 608.2241.

*4.1.5.9.4. N-(2-((2-(((S)-1-(4-hydroxyphenyl)ethyl)amino)-2-oxoethyl)thio)benzo[d] thiazol-6-yl)-2-methoxy-3-methyl-4-(pentan-2-yloxy)benzamide (**B21**).* White solid, 18.0% yield, ^{1}H NMR (400 MHz, $CDCl_3$) δ 10.05 (s, 1H), 8.14 (d, J = 1.8 Hz 1H), 8.05 (d, J = 8.8 Hz, 1H), 7.60 (d, J = 8.6 Hz, 1H), 7.35 (dd, J = 8.6, 1.8 Hz, 1H), 7.23 (d, J = 7.8 Hz, 1H), 6.86−6.73 (m, 4H), 6.41 (d, J = 8.4 Hz, 2H), 4.96 (quint, 1H), 4.50 (sext, 1H), 3.92 (brd, J = 14.7, 2H), 3.89 (s, 3H), 2.20 (s, 3H), 1.84−1.72 (m, 1H), 1.70−1.56 (m, 1H), 1.55−1.44 (m, 2H), 1.42 (d, J = 6.8 Hz, 3H), 1.34 (d, J = 6.0 Hz, 3H), 0.96 (t, J = 7.3 Hz, 3H). ^{13}C NMR (100 MHz, $CDCl_3$) δ 166.53, 164.90, 164.87, 160.98, 157.76, 155.49, 149.78, 136.40, 134.59, 133.75, 130.31, 126.93, 121.67, 121.58, 120.64, 116.99, 115.45, 115.16, 108.73, 74.14, 61.77, 48.70, 38.58, 36.15, 20.71, 19.76, 18.70, 14.07, 9.27. ESI-HRMS $[M+H]^+$ calcd for $C_{31}H_{35}N_3O_5S_2$: 594.2091, found: 594.2089.

*4.1.5.9.5. N-(2-((2-(((S)-1-(3-hydroxyphenyl)ethyl)amino)-2-oxoethyl)thio)benzo[d] thiazol-6-yl)-2-methoxy-3-methyl-4-(pentan-2-yloxy)benzamide (**B22**).* White solid, 25.0% yield, ^{1}H NMR (400 MHz, $CDCl_3$) δ 10.09 (s, 1H), 8.38 (s, 1H), 8.05 (d, J = 8.7 Hz, 1H), 7.76 (d, J = 7.3 Hz, 1H), 7.66 (d, J = 8.6 Hz, 1H), 7.38 (d, J = 8.6 Hz, 1H), 7.02 (t, J = 7.8 Hz, 1H), 6.80 (d, J = 8.9 Hz, 1H), 6.72 (d, J = 7.1 Hz, 1H), 6.60 (d, J = 12.7 Hz, 2H), 4.96 (quint, 1H), 4.50 (sext, 1H), 3.92 (brd, J = 14.7, 2H), 3.88 (s, 3H), 2.21 (s, 3H), 1.86−1.74 (m, 1H), 1.63−1.55 (m, 1H), 1.55−1.43 (m, 2H), 1.42 (d, J = 6.8 Hz, 3H), 1.35 (d, J = 6.0 Hz, 3H), 0.97 (t, J = 7.2 Hz, 3H). ^{13}C NMR (100 MHz, $CDCl_3$) δ 165.10, 162.88, 161.86, 158.57, 155.32, 154.22, 146.74, 142.03, 134.17, 133.05, 127.76, 127.24, 119.13, 118.35, 117.86, 115.52, 115.13, 112.32, 111.00, 106.58, 71.93, 59.57, 47.14, 36.30, 33.97, 19.25, 17.57, 16.51, 11.88, 7.06. ESI-HRMS $[M + H]^+$ calcd for $C_{31}H_{35}N_3O_5S_2$: 594.2091, found: 594.2094.

*4.1.5.9.6. N-(2-((2-(((S)-1-(2-hydroxyphenyl)ethyl)amino)-2-oxoethyl)thio)benzo[d] thiazol-6-yl)-2-methoxy-3-methyl-4-(pentan-2-yloxy)benzamide (**B23**).* White solid, 22.0% yield, ^{1}H NMR (400 MHz, $CDCl_3$) δ 10.13 (s, 1H), 8.77 (s, 1H), 8.60 (d, J = 2.0 Hz, 1H), 8.27 (d, J = 8.0 Hz, 1H), 8.05 (d, J = 8.8 Hz, 1H), 7.78 (d, J = 8.7 Hz, 1H), 7.45 (dd, J = 8.7, 2.1 Hz, 1H), 7.21−7.14 (m, 2H), 6.93 (d, J = 7.7 Hz, 1H), 6.85 (td, J = 7.5, 1.0 Hz, 1H), 6.81 (d, J = 9.0 Hz, 1H), 5.26 (quint, 1H), 4.50 (sext, 1H), 4.00 (d, J = 15.1 Hz, 1H), 3.90 (s, 3H), 3.86 (d, J = 15.0 Hz, 1H), 2.23 (s, 3H), 1.86−1.76 (m, 1H), 1.66−1.58 (m, 1H), 1.56−1.42 (m, 2H), 1.54 (d, J = 6.8 Hz, 3H), 1.36 (d, J = 6.1 Hz, 3H), 0.98 (t, J = 7.3 Hz, 3H). ^{13}C NMR (150 MHz, $CDCl_3$) δ 168.83, 164.06, 163.09, 160.14, 156.84, 154.36, 148.01, 136.04, 135.43, 129.51, 128.45, 127.82, 125.20, 120.60, 119.97, 119.65, 118.56, 117.54, 117.00, 111.64, 108.19, 73.52, 61.13, 43.21, 37.98, 35.34, 19.14, 18.63, 18.07, 13.43, 8.61. ESI-HRMS $[M+H]^+$ calcd for $C_{31}H_{35}N_3O_5S_2$: 594.2091, found: 594.2093.

*4.1.5.9.7. (S)-4-isobutoxy-2-methoxy-N-(2-((2-((1-(4-methoxyphenyl)ethyl)amino)-2- oxoethyl)thio) benzo [d]thiazol-6-yl)-3-methylbenzamide (**B24**).* White solid, 70.4% yield, ^{1}H NMR (400 MHz, DMSO-d_6) δ 10.31 (s, 1H), 8.69 (d, J = 8.0 Hz, 1H), 8.52 (s, 1H), 7.76 (d, J = 8.8 Hz, 1H), 7.68 (d, J = 8.7 Hz, 1H), 7.50 (d, J = 8.5 Hz, 1H), 7.22 (d, J = 8.4 Hz, 2H), 6.86 (d, J = 8.8 Hz, 1H), 6.82 (d, J = 8.6 Hz, 2H), 4.87 (quint, 1H), 4.13 (brd, J = 14.8 Hz, 2H), 3.81 (d, J = 6.2 Hz, 2H), 3.74 (s, 3H), 3.70 (s, 3H), 2.14 (s, 3H), 2.10–2.01 (m, 1H), 1.34 (d, J = 6.9 Hz, 3H), 1.00 (d, J = 6.6 Hz, 6H). ^{13}C NMR (150 MHz, $CDCl_3$) δ 166.51, 164.45, 162.99, 160.86, 158.09, 156.59, 148.13, 136.02, 135.33, 134.44, 129.69, 126.50, 120.63, 119.29, 118.33, 117.41, 113.29, 111.51, 107.10, 74.16, 61.18, 54.61, 48.17, 35.75, 27.73, 21.17, 18.62, 8.41. ESI-HRMS $[M+H]^+$ calcd for $C_{31}H_{35}N_3O_5S_2$: 594.2091, found: 594.2091.

*4.1.5.9.8. (S)-4-isopropoxy-2-methoxy-N-(2-((2-((1-(4-methoxyphenyl)ethyl)amino)- 2-oxoethyl)thio) benzo[d]thiazol-6-yl)-3-methylbenzamide (**B25**).* White solid, 68.5% yield, ^{1}H NMR (400 MHz, DMSO-d_6) δ 10.31 (s, 1H), 8.69 (d, J = 7.9 Hz, 1H), 8.52 (s, 1H), 7.75 (d, J = 8.8 Hz, 1H), 7.67 (d, J = 8.8 Hz, 1H), 7.47 (d, J = 8.4 Hz, 1H), 7.21 (d, J = 8.4 Hz, 2H), 6.88 (d, J = 8.8 Hz, 1H), 6.81 (d, J = 8.4 Hz, 2H), 4.86 (quint, 1H), 4.71–4.58 (m, 1H), 4.14 (brd, J = 14.8 Hz, 2H), 3.70 (d, J = 12.2 Hz, 6H), 2.09 (s, 3H), 1.33 (d, J = 6.9 Hz, 3H), 1.28 (d, J = 5.9 Hz, 6H). ^{13}C NMR (150 MHz, $CDCl_3$) δ 166.53, 164.43, 163.01, 159.86, 158.09, 156.84, 148.12, 136.02, 135.34, 134.44, 129.47, 126.50, 120.63, 120.02, 118.32, 117.18, 113.29, 111.51, 108.35, 69.96, 61.11, 54.61, 48.17, 35.75, 21.49, 21.17, 8.61. ESI-HRMS $[M+H]^+$ calcd for $C_{30}H_{33}N_3O_5S_2$: 580.1934, found: 580.1937.

*4.1.5.9.9. (S)-2,4-dimethoxy-N-(2-((2-((1-(4-methoxyphenyl) ethyl)amino)-2-oxoethyl) thio)benzo[d]thiazol-6-yl)-3-methylbenzamide (**B26**).* White solid, 65.0% yield, ^{1}H NMR (400 MHz, DMSO-d_6) δ 10.30 (s, 1H), 8.67 (d, J = 7.4 Hz, 1H), 8.49 (s, 1H), 7.73 (d, J = 8.8 Hz, 1H), 7.65 (d, J = 7.9 Hz, 1H), 7.49 (d, J = 8.4 Hz, 1H), 7.19 (d, J = 8.2 Hz, 2H), 6.86 (d, J = 8.6 Hz, 1H), 6.79 (d, J = 8.3 Hz, 2H), 4.84 (quint, 1H), 4.12 (brd, J = 14.8 Hz, 2H), 3.81 (s, 3H), 3.70 (s, 3H), 3.67 (s, 3H), 2.08 (s, 3H), 1.31 (d, J = 6.7 Hz, 3H). ^{13}C NMR (150 MHz, $CDCl_3$) δ 166.52, 164.49, 162.94, 161.28, 158.09, 156.56, 148.15, 136.02, 135.28, 134.43, 129.75, 126.50, 120.64, 119.23, 118.33, 117.74, 113.29, 111.53, 106.31, 61.20, 55.23, 54.62, 48.17, 35.75, 21.17, 8.40. ESI-HRMS $[M+H]^+$ calcd for $C_{28}H_{29}N_3O_5S_2$: 552.1621, found: 552.1617.

*4.1.6. General procedures for the synthesis of **B27–B30***

*4.1.6.1. 4-(benzyloxy)-2-hydroxy-3-methylbenzaldehyde (**22**).* To a solution of **21** (3.0 g, 19.72 mmol) in acetonitrile were added benzyl bromide (2.58 mL, 21.69 mmol), KI (327 mg, 1.972 mmol) and potassium carbonate (6.0 g, 43.38 mmol). The mixture was stirred at reflux for about 6 h and the completion of the reaction was monitored by TLC and LC-MS. After cooling to room temperature, the solvent was removed under reduced pressure. The residue was dissolved in ethyl acetate (100 mL), and washed with water and brine. Then the organic phase dried with sodium sulfate and concentrated *in vacuo*. The crude compound was purified by silica gel column chromatography (PE/EA = 15/1, v/v) to give **22** as a white solid (4.0 g , 88.2% yield). ^{1}H NMR (400 MHz, DMSO-d_6) δ 11.35 (s, 1H), 9.78 (s, 1H), 7.59 (d, J = 8.7 Hz, 1H), 7.43 (d, J = 7.5 Hz, 2H), 7.38 (t, J = 7.4 Hz, 2H), 7.31 (t, J = 7.2 Hz, 1H), 6.82 (d, J = 8.7 Hz, 1H), 5.23 (s, 2H), 2.02 (s, 3H). ESI-MS: calcd for $[M+H]^+$ m/z 231.1, found:231.1.

*4.1.6.2. 4-(benzyloxy)-2-methoxy-3-methylbenzaldehyde (**23**).* To a solution of **22** (3.0 g, 13.03 mmol) in anhydrous DMF were added CH_3I (3.25 mL, 52.12 mmol) and potassium carbonate (3.96 g, 28.67 mmol). The mixture was stirred at 40 °C for about 3 h and the completion of the reaction was monitored by TLC and LC-MS. After cooling to room temperature, water was added and the mixture was extracted with ethyl acetate (100 mL) twice. The combined organic layers were washed with brine and the organic phase was dried with sodium sulfate and concentrated *in vacuo*. Finally, the crude compound was purified by silica gel column chromatography (PE/EA = 10/1, v/v) to give **23** as a white solid (3.3 g, 98.9% yield). ^{1}H NMR (400 MHz, DMSO-d_6) δ 10.08 (s, 1H), 7.61 (d, J = 8.7 Hz, 1H), 7.44 (d, J = 7.4 Hz, 2H), 7.38 (t, J = 7.4 Hz, 2H), 7.31 (t, J = 7.2 Hz, 1H), 7.02 (d, J = 8.7 Hz, 1H), 5.21 (s, 2H), 3.78 (s, 3H), 2.11 (s, 3H). ESI-MS: calcd for $[M+H]^+$ m/z 257.1, found:257.1.

*4.1.6.3. 4-(benzyloxy)-2-methoxy-3-methylbenzoic acid (**24**).* To a solution of **23** (3.0 g, 11.7 mmol) in t-BuOH (30 mL) and 2-methyl-2-butene (10 mL) were added $NaClO_2$ (1.59 g, 17.55 mmol) and $NaH_2PO_4 \cdot 2H_2O$ (4.2 g, 35.1 mmol) buffer solution (pH = 4.5, 35 mL) at 0 °C. Then the mixture was stirred at room temperature for about 1 h. The solution was extracted with ethyl acetate (100 mL × 3) and the organic layer was dried with sodium sulfate and concentrated *in vacuo*. The crude compound was purified by silica gel column chromatography (DCM/CH_3OH = 10/1, v/v) to give **24** (3.18 g, 100% yield). ^{1}H NMR (400 MHz, DMSO-d_6) δ 12.04 (s, 1H), 7.60 (d, J = 8.7 Hz, 1H), 7.44 (d, J = 7.4 Hz, 2H), 7.38 (t, J = 7.5 Hz, 2H), 7.31 (t, J = 7.0 Hz, 1H), 6.88 (d, J = 8.7 Hz, 1H), 5.15 (s, 2H), 3.67 (s, 3H), 2.08 (s, 3H). ESI-MS: calcd for $[M-H]^-$ m/z 271.3, found: 271.3.

*4.1.6.4. 4-Hydroxy-2-methoxy-3-methylbenzoic acid (**25**).* A solution of compound **24** (3.0 g, 11.03 mmol) in methanol (30 mL) was hydrogenated in the presence of 10% Pd/C (300 mg) and H_2 (balloon pressure) at room temperature for 1 h. The mixture was then filtered through a Celite pad and the filtrate was concentrated *in vacuo* to give **25,** which was used directly for the following synthesis. ESI-MS: calcd for $[M-H]^-$ m/z 181.1, found: 181.2.

*4.1.6.5. Methyl 4-hydroxy-2-methoxy-3-methylbenzoate (**26**).* $SOCl_2$ (796 μL, 10.98 mmol) was slowly added to a solution of **26** (2.0 g, 10.98 mmol) in dry methanol (25 mL) and the solution was stirred at rt for 5 h. After removing the solvent under reduced pressure, the residue was dissolved in ethyl acetate (50 mL), washed with water and brine. Then the organic phase was dried with sodium sulfate and concentrated *in vacuo*. The crude compound was purified by silica gel column chromatography (PE/EA = 6/1, v/v) to give **26** as a white solid (2.1 g , 98.0% yield) . ^{1}H NMR (400 MHz, DMSO-d_6) δ 10.24 (s, 1H), 7.47 (d, J = 8.6 Hz, 1H), 6.62 (d, J = 8.6 Hz, 1H), 3.72 (s, 3H), 3.65 (s, 3H), 2.00 (s, 3H). ESI-MS: calcd for $[M+H]^+$ m/z 197.1, found:197.1.

*4.1.6.6. General procedures for the synthesis of **27a-27d**.* To a solution of **26** (196 mg, 1.0 mmol) in anhydrous DMF were added different alkyl halides (278 mg, 2.0 mmol, 1-bromo-2-methoxyethane for **27a**, 340 mg, 2.0 mmol, 1-(2-chloroethyl)pyrrolidine hydrochloride for **27b**, 288 mg, 2.0 mmol, 2-chloro-N,N-dimethylethan-1-amine hydrochloride for **27c**, 372 mg, 2.0 mmol, 4-(2-chloroethyl)morpholine hydrochloride for **27d**), KI (16.6 mg, 0.1 mmol) and potassium carbonate (414 mg, 3.0 mmol). The mixture was stirred at 100 °C for about 2 h and the completion of the reaction was monitored by TLC and LC-MS. After cooling to room temperature, water was added. The mixture was extracted with ethyl acetate (20 mL) twice. The combined organic layers were washed with brine and the organic phase was dried with sodium sulfate and concentrated *in vacuo*. The crude compound was purified by silica gel column chromatography (PE/EA = 10/1, v/v) to give **27a-27d**.

*4.1.6.6.1. Methyl 2-methoxy-4-(2-methoxyethoxy)-3-methylbenzoate (**27a**).* Brown oil, 93.5% yield, ^{1}H NMR (400 MHz, DMSO-d_6) δ 7.59 (d, J = 8.8 Hz, 1H), 6.81 (d, J = 8.8 Hz, 1H), 4.14–4.10

(m, 2H), 3.75 (s, 3H), 3.68–3.63 (m, 5H), 3.29 (s, 3H), 2.04 (s, 3H). ESI-MS: calcd for $[M+H]^+$ *m/z* 255.1, found:255.2.

*4.1.6.6.2. Methyl 2-methoxy-3-methyl-4-(2-(pyrrolidin-1-yl) ethoxy)benzoate (**27b**).* Brown oil, 41.9% yield, ^{1}H NMR (400 MHz, $CDCl_3$) δ 7.72 (d, J = 8.7 Hz, 1H), 6.63 (d, J = 8.7 Hz, 1H), 4.15 (t, J = 5.9 Hz, 2H), 3.87 (s, 3H), 3.79 (s, 3H), 2.94 (t, J = 5.9 Hz, 2H), 2.70–2.62 (m, 4H), 2.15 (s, 3H), 1.84–1.76 (m, 4H). ESI-MS: calcd for $[M+H]^+$ *m/z* 294.2, found:294.2.

*4.1.6.6.3. Methyl 4-(2-(dimethylamino)ethoxy)-2-methoxy-3-methylbenzoate (**27c**).* Brown oil, 84.3% yield, ^{1}H NMR (400 MHz, DMSO-d_6) δ 7.59 (d, J = 8.8 Hz, 1H), 6.81 (d, J = 8.8 Hz, 1H), 4.07 (t, J = 5.7 Hz, 2H), 3.75 (s, 3H), 3.66 (s, 3H), 2.63 (t, J = 5.6 Hz, 2H), 2.20 (s, 6H), 2.03 (s, 3H). ESI-MS: calcd for $[M+H]^+$ *m/z* 268.2, found:268.1.

*4.1.6.6.4. Methyl 2-methoxy-3-methyl-4-(2-morpholinoethoxy) benzoate (**27d**).* Brown oil, 90.5% yield, ^{1}H NMR (400 MHz, DMSO-d_6) δ 7.60 (d, J = 8.7 Hz, 1H), 6.83 (d, J = 8.8 Hz, 1H), 4.12 (t, J = 5.7 Hz, 2H), 3.75 (s, 3H), 3.66 (s, 3H), 3.57–3.51 (m, 4H), 2.70 (t, J = 5.7 Hz, 2H), 2.03 (s, 3H). ESI-MS: calcd for $[M+H]^+$ *m/z* 310.1, found:310.2.

*4.1.6.7. 2-Methoxy-4-(2-methoxyethoxy)-3-methylbenzoic acid (**28a**).* Compound **28a** was prepared in a similar manner as described for compound **9c**, starting from 2**7a** (139 mg, 0.545 mmol). The residue was purified by flash column chromatography on silica gel (200–300 mesh) using dichloromethane/methanol eluent (DCM/CH_3OH = 10/1, v/v) to afford the desired product as white solid (131 mg, 100.0% yield). ^{1}H NMR (400 MHz, DMSO-d_6) δ 7.59 (d, J = 8.7 Hz, 1H), 6.79 (d, J = 8.7 Hz, 1H), 4.15–4.07 (m, 2H), 3.67–3.63 (m, 5H), 3.29 (s, 3H), 2.04 (s, 3H). ESI-MS: calcd for $[M-H]^-$ *m/z* 239.1, found:239.1.

*4.1.6.8. General procedures for the synthesis of **28b**-**28d**.* 6 M HCl aqueous solution (5 mL) was added to **27b**-**27d** (0.545 mmol) and the solution was stirred at 80 °C for about 6 h. After solvent evaporation under reduced pressure, the residue was used for the following synthesis.

*4.1.6.9. General procedures for the synthesis of **29a**-**29d**.* Compounds **29a**-**29d** were prepared in a similar manner as described for compounds **20a**-**20d**, starting from **28a**-**28d** (0.50 mmol).

*4.1.6.10. General procedures for the synthesis of **B27**–**B30**.* The syntheses of the products **B27**–**B30** from **29a**-**29d** (0.24 mmol) and **14a** (74.7 mg, 0.20 mmol) were similar to the previously reported method published in ref. 32. The residues were purified by flash column chromatography on silica gel (200–300 mesh) using dichloromethane/methanol eluent (DCM/CH_3OH = 10/1, v/v) to afford the desired products.

*4.1.6.10.1. (S)-2-methoxy-4-(2-methoxyethoxy)-N-(2-((2-((1-(4-methoxyphenyl)ethyl) amino)-2-oxoethyl)thio)benzo[d]thiazol-6-yl)-3-methylbenzamide (**B27**).* White solid, 35.0% yield, ^{1}H NMR (400 MHz, DMSO-d_6) δ 10.33 (s, 1H), 8.69 (d, J = 8.0 Hz, 1H), 8.53 (d, J = 1.8 Hz, 1H), 7.77 (d, J = 8.8 Hz, 1H), 7.69 (dd, J = 8.9, 2.0 Hz, 1H), 7.51 (d, J = 8.6 Hz, 1H), 7.23 (d, J = 8.6 Hz, 2H), 6.90 (d, J = 8.7 Hz, 1H), 6.83 (d, J = 8.7 Hz, 2H), 4.93–4.83 (m, 1H), 4.20–4.13 (m, 4H), 3.75 (s, 3H), 3.73–3.69 (m, 5H), 3.34 (s, 3H), 2.14 (s, 3H), 1.35 (d, J = 7.0 Hz, 3H). ^{13}C NMR (100 MHz, DMSO-d_6) δ 165.77, 165.27, 164.91, 159.88, 158.53, 157.08, 149.27, 136.60, 136.55, 135.86, 128.34, 127.59, 122.52, 121.44, 119.77, 119.65, 114.05, 112.32, 107.88, 70.86, 68.35, 62.01, 58.85, 55.51, 48.31, 37.23, 22.84, 9.41. ESI-HRMS $[M+H]^+$ calcd for $C_{30}H_{33}N_3O_6S_2$: 596.1884, found: 596.1887.

*4.1.6.10.2. (S)-2-methoxy-N-(2-((2-((1-(4-methoxyphenyl)ethyl) amino)-2-oxoethyl)thio) benzo[d]thiazol-6-yl)-3-methyl-4-(2-(pyrrolidin-1-yl)ethoxy)benzamide (**B28**).* White solid, 35.0% yield, ^{1}H NMR (400 MHz, $CDCl_3$) δ 9.94 (s, 1H), 8.49 (d, J = 1.7 Hz, 1H), 7.98 (d, J = 8.8 Hz, 1H), 7.72 (d, J = 7.6 Hz, 1H), 7.60 (d, J = 8.7 Hz, 1H), 7.33 (dd, J = 8.7, 1.9 Hz, 1H), 7.06 (d, J = 8.6 Hz, 2H), 6.74 (d, J = 8.9 Hz, 1H), 6.67 (d, J = 8.6 Hz, 2H), 4.99–4.90 (m, 1H), 4.34 (t, J = 5.0 Hz, 2H), 3.85 (brd, J = 14.7, 2H), 3.80 (s, 3H), 3.67 (s, 3H), 3.24 (t, J = 5.0 Hz, 2H), 3.08–3.02 (m, 4H), 2.16 (s, 3H), 2.00–1.92 (m, 4H), 1.34 (d, J = 6.8 Hz, 3H). ^{13}C NMR (100 MHz, $CDCl_3$) δ 167.17, 165.20, 163.34, 160.21, 158.70, 157.28, 148.83, 136.64, 135.78, 135.05, 130.54, 127.13, 121.27, 119.84, 119.17, 118.98, 113.91, 112.21, 107.82, 65.67, 61.93, 55.26, 54.60, 54.24, 48.81, 36.37, 23.40, 21.82, 9.32. ESI-HRMS $[M+H]^+$ calcd for $C_{33}H_{38}N_4O_5S_2$: 635.2356, found: 635.2358.

*4.1.6.10.3. (S)-4-(2-(dimethylamino)ethoxy)-2-methoxy-N-(2-((2-((1-(4-methoxyphenyl) ethyl)amino)-2-oxoethyl)thio)benzo[d]thiazol-6-yl)-3-methylbenzamide (**B29**).* White solid, 32.0% yield, ^{1}H NMR (400 MHz, DMSO-d_6) δ 10.34 (s, 1H), 8.72 (d, J = 8.0 Hz, 1H), 8.52 (s, 1H), 7.78 (d, J = 8.8 Hz, 1H), 7.69 (dd, J = 8.8, 1.5 Hz, 1H), 7.52 (d, J = 8.6 Hz, 1H), 7.23 (d, J = 8.6 Hz, 2H), 6.91 (d, J = 8.7 Hz, 1H), 6.83 (d, J = 8.6 Hz, 2H), 4.92–4.82 (m, 1H), 4.20–4.07 (m, 4H), 3.74 (s, 3H), 3.71 (s, 3H), 2.72 (t, J = 5.5 Hz, 2H), 2.27 (s, 6H), 2.13 (s, 3H), 1.35 (d, J = 6.9 Hz, 3H). ^{13}C NMR (100 MHz, DMSO-d_6) δ 165.86, 165.29, 164.95, 159.88, 158.50, 157.06, 149.27, 136.53, 135.86, 128.42, 127.58, 122.26, 121.46, 119.68, 114.03, 112.36, 107.71, 67.08, 62.02, 57.96, 55.49, 48.34, 45.96, 37.18, 22.81, 9.40. ESI-HRMS $[M+H]^+$ calcd for $C_{31}H_{36}N_4O_5S_2$: 609.2200, found: 609.2195.

*4.1.6.10.4. (S)-2-methoxy-N-(2-((2-((1-(4-methoxyphenyl)ethyl) amino)-2-oxoethyl) thio)benzo[d]thiazol-6-yl)-3-methyl-4-(2-morpholinoethoxy)benzamide (**B30**).* White solid, 30.0% yield, ^{1}H NMR (400 MHz, $CDCl_3$) δ 9.93 (s, 1H), 8.49 (d, J = 2.0 Hz, 1H), 7.99 (d, J = 8.8 Hz, 1H), 7.71 (d, J = 7.6 Hz, 1H), 7.60 (d, J = 8.7 Hz, 1H), 7.33 (dd, J = 8.7, 2.1 Hz, 1H), 7.06 (d, J = 8.6 Hz, 2H), 6.75 (d, J = 8.9 Hz, 1H), 6.67 (d, J = 8.7 Hz, 2H), 4.99–4.90 (m, 1H), 4.37 (t, J = 4.5 Hz, 2H), 3.92–3.82 (m, 6H), 3.81 (s, 3H), 3.67 (s, 3H), 3.14 (t, J = 4.5 Hz, 2H), 2.99–2.87 (m, 4H), 2.15 (s, 3H), 1.35 (d, J = 6.9 Hz, 3H). ^{13}C NMR (100 MHz, $CDCl_3$) δ 167.19, 165.26, 163.29, 158.71, 157.31, 148.86, 136.65, 135.73, 135.04, 130.58, 127.14, 121.29, 119.85, 118.98, 113.91, 112.23, 107.84, 65.24, 61.95, 57.09, 55.26, 53.40, 48.82, 36.36, 21.81, 9.31. ESI-HRMS $[M+H]^+$ calcd for $C_{33}H_{38}N_4O_6S_2$: 651.2306, found: 651.2315.

*4.1.7. General procedures for the synthesis of **B31***

*4.1.7.1. Tert-butyl (S)-(2-((1-(4-methoxyphenyl)ethyl)amino)-2-oxoethyl)carbamate (**31**).* To a solution of (*tert*-butoxycarbonyl) glycine (1.0 g, 5.7 mmol) in anhydrous THF (30 mL) were added HATU (2.17 g, 5.7 mmol) and HOAT (776 mg, 5.7 mmol) at 0 °C for 15 min. Then (S)-1-(4-methoxyphenyl)ethan-1-amine (860 mg, 5.7 mmol) and DIPEA (3.0 mL, 17.1 mmol) were added. The mixture was stirred at room temperature for about 8 h and the completion of the reaction was monitored by TLC. Then the aqueous layer was extracted with ethyl acetate (100 mL) twice, and the combined organic layers were washed with brine, dried over sodium sulfate, and concentrated under reduced pressure. The residue was purified by column chromatography on silica gel (PE/EA = 10/1, v/v) to afford intermediate **31** (colorless oil, 92.8% yield). ^{1}H NMR (600 MHz, $CDCl_3$) δ 7.22 (d, J = 8.6 Hz, 2H), 6.85 (d, J = 8.7 Hz, 2H), 6.58 (s, 1H), 5.33 (s, 1H), 5.12–5.00 (m, 1H), 3.78 (s, 3H), 3.75 (d, J = 4.2 Hz, 2H), 1.46 (d, J = 6.9 Hz, 3H), 1.43 (s, 9H). ESI-MS: calcd for $[M+Na]^+$ *m/z* 331.2, found:331.0.

*4.1.7.2. (S)-2-amino-N-(1-(4-methoxyphenyl)ethyl)acetamide (**32**).* To a solution of **31** (1.0 g, 3.25 mmol) in anhydrous CH_2Cl_2 (15 mL)

was added trifluoroacetic acid (1.5 mL) at 0 °C and stirred for 3 h. After removal of the solvents under reduced pressure, saturated sodium bicarbonate solution and CH_2Cl_2 were added. The organic layer was washed with brine, dried with sodium sulfate and concentrated *in vacuo* to give the crude product, which was used directly for the next step. ESI-MS: calcd for $[M + H]^+$ *m/z* 209.1, found:209.2.

*4.1.7.3. (S)—N-(1-(4-methoxyphenyl)ethyl)-2-((6-nitrobenzo[d]thiazol-2-yl)amino) acetamide (**33**).* To a solution of 2-chloro-6-nitrobenzo [*d*]thiazole (114 mg, 0.53 mmol) in n-butyl alcohol (5 mL) were added **32** (110 mg, 0.53 mmol) and Et_3N (242 μL, 1.75 mmol) at 0 °C. The mixture was stirred at reflux for about 3 h and the completion of the reaction was monitored by TLC. Reducing temperature led to a precipitation of compound **33**, which was filtered and dried (yellow solid, 73.5% yield). ^{1}H NMR (600 MHz, DMSO-d_6) δ 8.97 (t, J = 5.5 Hz, 1H), 8.72 (d, J = 2.3 Hz, 1H), 8.51 (d, J = 8.0 Hz, 1H), 8.13 (dd, J = 8.9, 2.4 Hz, 1H), 7.47 (d, J = 8.9 Hz, 1H), 7.26 (d, J = 8.6 Hz, 2H), 6.87 (d, J = 8.6 Hz, 2H), 4.96—4.88 (m, 1H), 4.14 (d, J = 5.1 Hz, 2H), 3.72 (s, 3H), 1.36 (d, J = 6.9 Hz, 3H). ESI-MS: calcd for $[M + H]^+$ *m/z* 387.1, found:387.2.

*4.1.7.4. (S)-2-((6-aminobenzo[d]thiazol-2-yl)amino)-N-(1-(4-methoxyphenyl)ethyl) acetamide (**34**).* To a solution of **33** (150 mg, 0.39 mmol) in CH_3CH_2OH/H_2O (10 mL/5 mL) were added Fe powder (109 mg, 1.95 mmol) and NH_4Cl (104 mg, 1.95 mmol) at room temperature. The mixture was stirred at reflux for about 3 h and the completion of the reaction was monitored by TLC. After cooling and filtration on Celite, the mixture was extracted with ethyl acetate (20 mL × 3) and the combined organic solvents were washed with water. The organic layer was dried with sodium sulfate and concentrated *in vacuo* to give the crude product, which was used directly for the next step. ESI-MS: calcd for $[M+H]^+$ *m/z* 357.1, found:357.2.

*4.1.7.5. (S)-2,4-dimethoxy-N-(2-((2-((1-(4-methoxyphenyl)ethyl) amino)-2-oxoethyl) amino)benzo[d]thiazol-6-yl)-3-methylbenzamide (**B31**).* The synthesis of the product **B31** from **20d** (51.5 mg, 0.24 mmol) and **34** (71.3 mg, 0.20 mmol) was similar to the previously reported method published in ref. 32. The residue was purified by flash column chromatography on silica gel (200—300 mesh) using petroleum ether/ethyl acetate eluent (PE/EA = 3/1, v/v) to afford the desired product as white solid (80.2 mg, 75.0% yield). ^{1}H NMR (400 MHz, DMSO-d_6) δ 10.10 (s, 1H), 8.43 (d, J = 8.2 Hz, 1H), 8.19 (dd, J = 11.1, 3.8 Hz, 2H), 7.52 (d, J = 8.6 Hz, 1H), 7.48 (dd, J = 8.7, 1.9 Hz, 1H), 7.34 (d, J = 8.6 Hz, 1H), 7.26 (d, J = 8.6 Hz, 2H), 6.89 (d, J = 8.7 Hz, 1H), 6.85 (d, J = 8.7 Hz, 2H), 4.96—4.86 (m, 1H), 4.03 (d, J = 5.8 Hz, 2H), 3.85 (s, 3H), 3.74 (s, 3H), 3.72 (s, 3H), 2.12 (s, 3H), 1.35 (d, J = 7.0 Hz, 3H). ^{13}C NMR (150 MHz, DMSO-d_6) δ 167.58, 165.40, 164.10, 159.82, 157.82, 156.27, 148.32, 136.24, 132.97, 130.73, 127.77, 126.98, 121.86, 118.70, 118.11, 117.62, 113.38, 112.08, 106.15, 61.34, 55.71, 54.88, 47.10, 46.45, 22.29, 8.71. ESI-HRMS $[M+H]^+$ calcd for $C_{28}H_{30}N_4O_5S$: 535.2010, found: 535.2010.

*4.1.8. General procedures for the synthesis of **B32***

*4.1.8.1. N-(2-chlorobenzo[d]thiazol-6-yl)-2,4-dimethoxy-3-methylbenzamide (**36**).* Compounds **36** was prepared in a similar manner as described for compound **B1**—**B14**, starting from 2-chlorobenzo [*d*]thiazol-6-amine (**35**, 923 mg, 5.0 mmol) and **20d** (1.29 g, 6.0 mmol). The residue was purified by flash column chromatography on silica gel (200—300 mesh) using petroleum ether/ethyl acetate eluent (PE/EA = 10/1, v/v) to afford the desired product (1.27 g, 70.0% yield). ^{1}H NMR (400 MHz, $CDCl_3$) δ 10.12 (s, 1H), 8.68 (d, J = 2.1 Hz, 1H), 8.06 (d, J = 8.8 Hz, 1H), 7.36 (dd, J = 8.8, 2.2 Hz, 1H), 6.80 (d, J = 8.8 Hz, 2H), 3.90 (s, 3H), 3.86 (s, 3H), 2.21 (s, 3H). ESI-MS: calcd for $[M+H]^+$ *m/z* 363.0, found:363.1.

*4.1.8.2. N-(2-chlorobenzo[d]thiazol-6-yl)-2,4-dimethoxy-3-methylbenzamide (**37**).* To a solution of **36** (363 mg, 1.0 mmol) in anhydrous THF were added ethyl 2-hydroxyacetate (257 mg, 1.2 mmol) and NaH (60 mg, 1.5 mmol, 60% dispersion in mineral oil). The mixture was stirred at reflux for about 2 h and the completion of the reaction was monitored by TLC. After adding water (2 mL), the mixture was extracted with ethyl acetate (10 mL × 3). Then the organic phase was dried with sodium sulfate and concentrated *in vacuo* to give the crude product, which was purified by silica gel column chromatography (PE/EA = 6/1, v/v) to obtain compound **37** as colorless oil (278 mg, 64.6% yield). ^{1}H NMR (400 MHz, $CDCl_3$) δ 9.98 (s, 1H), 8.44 (d, J = 2.1 Hz, 1H), 8.07 (d, J = 8.8 Hz, 1H), 7.62 (d, J = 8.6 Hz, 1H), 7.35 (dd, J = 8.7, 2.2 Hz, 1H), 6.81 (d, J = 8.9 Hz, 1H), 5.08 (s, 2H), 4.29 (q, J = 7.1 Hz, 2H), 3.90 (s, 3H), 3.86 (s, 3H), 2.21 (s, 3H), 1.30 (t, J = 7.1 Hz, 3H). ESI-MS: calcd for $[M + H]^+$ *m/z* 431.1, found: 431.1.

*4.1.8.3. 2-((6-(2,4-dimethoxy-3-methylbenzamido)benzo[d]thiazol-2-yl)oxy)acetic acid (**38**).* The compound **37** (270 mg, 0.63 mmol) was stirred in NaOH (1 M) water solution (5 mL) and THF (5 mL) for 5 min. Then the THF was removed under vacuum, and the residue was acidified to pH = 2 or below with HCl (1 M). Then the solution was extracted with ethyl acetate (20 mL × 3) and the combined organic solvents were dried with sodium sulfate and concentrated *in vacuo*. The crude product was used directly for next step. ESI-MS: calcd for $[M - H]^-$ *m/z* 401.1, found:401.1.

*4.1.8.4. (S)-2,4-dimethoxy-N-(2-(2-((1-(4-methoxyphenyl)ethyl) amino)-2-oxoethoxy) benzo[d]thiazol-6-yl)-3-methylbenzamide (**B32**).* The synthesis of the product **B32** from **11b** (30.2 mg, 0.20 mmol) and **38** (80.5 mg, 0.20 mmol) was similar to the previously reported method published in ref. 32. The residue was purified by flash column chromatography on silica gel (200—300 mesh) using petroleum ether/ethyl acetate eluent (PE/EA = 3/1, v/v) to afford the desired product as white solid (93.1 mg, 87.0% yield). ^{1}H NMR (400 MHz, DMSO-d_6) δ 10.26 (s, 1H), 8.63 (d, J = 8.1 Hz, 1H), 8.41 (s, 1H), 7.66—7.58 (m, 2H), 7.53 (d, J = 8.6 Hz, 1H), 7.26 (d, J = 8.6 Hz, 2H), 6.90 (d, J = 8.7 Hz, 1H), 6.86 (d, J = 8.7 Hz, 2H), 5.05—4.86 (m, 3H), 3.85 (s, 3H), 3.74 (s, 3H), 3.72 (s, 3H), 2.12 (s, 3H), 1.37 (d, J = 7.0 Hz, 3H). ^{13}C NMR (150 MHz, DMSO-d_6) δ 170.73, 165.00, 164.49, 159.93, 157.88, 156.31, 144.34, 135.97, 135.28, 131.82, 127.77, 127.00, 121.82, 120.33, 118.77, 113.40, 112.52, 106.17, 68.75, 61.38, 55.73, 54.88, 46.96, 22.06, 8.70. ESI-HRMS $[M+H]^+$ calcd for $C_{28}H_{29}N_3O_6S$: 536.1850, found: 536.1846.

4.2. Biological evaluation

4.2.1. Luciferase report assay

4.2.1.1. Cell lines culture. HepG2 cells were stably transfected with corresponding STAT-responsive firefly luciferase reporter plasmid and were cultured in a-MEM supplemented with 10% FBS, penicillin (100 U/mL), and streptomycin (100 μg/mL). HEK-293 cells were stably transfected with NF-κB-responsive firefly luciferase reporter plasmid and were cultured in DMEM supplemented with 10% FBS, penicillin (100 U/mL), and streptomycin (100 μg/mL). All the cell lines were incubated at 37 °C in a humidified atmosphere containing 5% CO_2.

4.2.1.2. Luciferase report assay. Procedure was similar to the published method in ref.32.

4.2.2. Cell viability assays

4.2.2.1. Cell lines culture. MDA-MB-468 cell lines were cultured in DMEM/F-12 supplemented with 10% (v/v) fetal bovine serum, 50 mg/mL penicillin/streptomycin. HEL cell lines were maintained in high glucose DMEM replenished with 10% fetal bovine serum and 50 mg/mL penicillin/streptomycin. All the cell lines were incubated at 37 °C in a humidified atmosphere containing 5% CO_2.

4.2.2.2. MTT assay. Procedure was similar to published methods in ref. [49].

4.2.3. Western blotting

Cells were collected and lysed using pre-heated 2% SDS by vortexing for 2–3 s at maximum speed, followed by boiling for 30 min. Protein concentrations were determined by BCA assay (Beyotime, P0011). Proteins were subjected to SDS-PAGE, transferred to nitrocellulose membranes (Immobilon-P, Millipore) and blocked for 1 h at room temperature with 3% milk in 1xTris-buffered saline Tween-20 (TBST) (25 mM Tris, 150 mM NaCl, 2 mM KCl, pH 7.4, supplemented with 0.1% Tween-20).

Membranes were probed with a 1:1000 dilution of primary antibodies (Cell Signaling Technology) against Phospho-STAT3 (Tyr705), Phospho-STAT3 (Ser727), STAT3, c-Myc, MCL-1, β-actin and GAPDH at 4 °C overnight. After washing the membranes with TBST three times for 30 min, horseradish peroxidase-conjugated anti-rabbit IgG (dilution, 1: 2000) or anti-mouse IgG (dilution, 1: 5000) antibodies were incubated at room temperature for 1 h. The membranes were washed with TBST three times for 30 min, and the antigen-antibody reaction was visualized with an enhanced chemiluminescence assay (Thermo Scientific) or Femto chemiluminescence assay (Thermo Scientific).

4.2.4. In vitro kinases activities test

For the kinase assay based on the ELISA system, procedure was similar to published methods in ref. [50] and ref.[51].

4.2.5. Flow cytometry analysis of apoptotic cells

Cells were seeded in 12-well plates for overnight and then treated with DMSO or the indicated compounds for 48 h. Then cells were collected and rinsed twice with PBS. After resuspending the cells in 500 μL binding buffer, 5 μL Annexin V-FITC and 5 μL propidium iodide (A211-01, Vazyme) were added and mixed gently. Finally, the mixture was incubated for 15 min at room temperature in dark and detected by a flow cytometer (BD FACs Calibur).

4.2.6. Cell cycle effect

Cells were seeded in 12-well plates overnight and then treated with DMSO or the indicated compounds for 48 h. The cells were washed with PBS and fixed in ice-cold 80% ethanol overnight. For analysis, cells were incubated for 30 min at 37 °C with PI (ST512, Beyotime Biotechnology)-containing RNase (B600476-0001, Sangon Biotech) and detected by a flow cytometer (BD FACS CALIBUR).

4.2.7. Surface plasmon resonance analysis

Purified STAT3 protein (His-tag 127–722 amino acid, DetaiBio, China) was immobilized on sensor chip CM5 (GE Healthcare) and carried out at 25 °C on Biacore T200 instruments. Approximately 11269.8 RU of STAT3 was amino coupled to a CM5 Chip (according to the manufacturer's protocol), and another cell being left blank for reference subtraction. HBS-EP buffer (0.01 M HEPES, 0.15 M NaCl, 3 mM EDTA, 0.05% v/v Surfactant P20, pH 7.4) was used as running buffer. The operating conditions: contact time: 30 s, flow rate: 30 μL/min, dissociation time: 45 s. The regeneration conditions: contact time: 30 s, flow rate: 30 μL/min. The ratio of the association and dissociation rate constants was determined as the affinity (equilibrium constants, K_D). The K_D (equilibrium constant) values were calculated as k_d (dissociation rate constant)/k_a (associated rate constant) for each interaction and determined by globally fitting with Biacore T200 evaluation software 2.0 (GE Healthcare).

4.2.8. Fluorescence polarization assay

Procedure was similar to the published method in ref. 48. Before adding tested compounds, the 5-FAM-GpYLPQTV-NH2 probe was incubated with STAT3 SH2 domain protein in assay buffer (Hepes 10 mM , pH = 7.5 , EDTA 1 mM , NaCl 50 mM , 0.1% Nonidet P40) for 30 min at 37 °C. Then, competition experiments were performed using different concentrations of compounds. The binding rate was calculated with the following formula: binding rate (%) = (maximum value - drug treatment value)/(maximum value - minimum value) × 100%.

4.2.9. Molecular docking

The X-ray crystal structure of STAT3/DNA complex (PDB code: 1BG1) was used for docking studies applying Schrodinger software package. Firstly, one monomer was deleted and the missing hydrogen atoms were added. Also, the bond order and the correct protonation were prepared using protein preparation wizard model. Then the complex was submitted to a series of restrained minimizations to relieve static clashes using the OPLS-2005 force field. Subsequently, the receptor grid was generated at the centroid of selected residues (Gln644, Glu638) and the size of grid box was 20 Å × 20 Å × 20 Å. After preparing the ligands, molecular docking was carried out using the standard precision (SP) with the default settings. Finally, the pictures were generated using Pymol software.

Declaration of competing interest

The authors declare that they have no known competing financial interests or personal relationships that could have appeared to influence the work reported in this paper.

Acknowledgement

Financial support was generously provided by the Significant New Drugs Development (2018ZX09711002-003-009), the National Natural Science Foundation of China (Nos. 81973178 and U1906212).

Appendix A. Supplementary data

Supplementary data to this article can be found online at https://doi.org/10.1016/j.ejmech.2021.113333.

References

[1] T. Bowman, R. Garcia, J. Turkson, et al., STATs in oncogenesis, Oncogene 21 (2000) 2474–2488.
[2] J.E. Darnell Jr., Transcription factors as targets for cancer therapy, Nat. Rev. Canc. 2 (2002) 740–749.
[3] E. James, Darnell Jr., STATs and gene regulation, Science 277 (1997) 1630–1635.
[4] J.N. Ihle, B.A. Witthuhn, F.W. Quelle, K. Yamamoto, O. Silvennoinen, Signaling through the hematopoietic cytokine receptors, Annu. Rev. Immunol. 13 (1997) 369–398.
[5] Y. Wang, A.H. van Boxel-Dezaire, H. Cheon, J. Yang, G.R. Stark, STAT3 activation in response to IL-6 is prolonged by the binding of IL-6 receptor to EGF receptor, Proc. Natl. Acad. Sci. U.S.A. 110 (2013) 16975–16980.
[6] J. Turkson, D. Ryan, J.S. Kim, Y. Zhang, Z. Chen, E. Haura, A. Laundano, S. Sebti, A.D. Hamilton, R. Jove, Phosphotyrosyl peptides block Stat3-mediated DNA binding activity, gene regulation, and cell transformation, J. Biol. Chem. 276 (2001) 45443–45455.
[7] W.S. Alexander, Suppressors of cytokine signalling (SOCS) in the immune system, Nat. Rev. Immunol. 2 (2002) 410–416.

[8] M. Kubo, T. Hanada, A. Yoshimura, Suppressors of cytokine signaling and immunity, Nat. Immunol. 4 (2003) 1169–1176.
[9] K. Shuai, B. Liu, Regulation of gene-activation pathways by PIAS proteins in the immune system, Nat. Rev. Immunol. 5 (2005) 593–605.
[10] J.E. Darnell, Validating Stat3 in cancer therapy, Nat. Med. 11 (2005) 595–596.
[11] R. Buettner, L.B. Mora, R. Jove, Activated STAT signaling in human tumors provides novel molecular targets for therapeutic intervention, Clin. Canc. Res. 8 (2002) 945–954.
[12] J. Turkson, R. Jove, STAT proteins: novel molecular targets for cancer drug discovery, Oncogene 19 (2000) 6613–6626.
[13] J. Turkson, STAT proteins as novel targets for cancer drug discovery, Expert Opin. Ther. Targets 8 (2004) 409–422.
[14] H. Yu, R. Jove, The STATs of cancer: new molecular targets come of age, Nat. Rev. Canc. 4 (2004) 97–105.
[15] H. Yu, D. Pardoll, R. Jove, STATs in cancer inflammation and immunity: a leading role for STAT3, Nat. Rev. Canc. 9 (2009) 798–809.
[16] A. Herrmann, M. Kortylewski, M. Kujawski, C. Zhang, K. Reckamp, B. Armstrong, L. Wang, C. Kowolik, J. Deng, R. Figlin, H. Yu, Targeting Stat3 in the myeloid compartment drastically improves the in vivo antitumor functions of adoptively transferred T cells, Canc. Res. 70 (2010) 7455–7464.
[17] M. Kortylewski, H. Yu, Role of Stat3 in suppressing anti-tumor immunity, Curr. Opin. Immunol. 20 (2008) 228–233.
[18] M. Kortylewski, M. Kujawski, T. Wang, S. Wei, S. Zhang, S. Pilon-Thomas, G. Niu, H. Kay, J. Mulé, W.G. Kerr, R. Jove, D. Pardoll, H. Yu, Inhibiting Stat3 signaling in the hematopoietic system elicits multicomponent antitumor immunity, Nat. Med. 11 (2005) 1314–1321.
[19] H. Yu, M. Kortylewski, D. Pardoll, Crosstalk between cancer and immune cells: role of STAT3 in the tumour microenvironment, Nat. Rev. Immunol. 7 (2007) 41–51.
[20] N. Kumari, B. Dwarakanath, A. Das, A.N. Bhatt, Role of interleukin-6 in cancer progression and therapeutic resistance, Tumor Biol. 37 (2016) 11553–11572.
[21] T. Gharibi, Z. Babaloo, A. Hosseini, M. Abdollahpour-Alitappeh, V. Hashemi, F. Marofi, K. Nejati, B. Baradaran, Targeting STAT3 in cancer and autoimmune diseases, Eur. J. Pharmacol. 878 (2020) 173107.
[22] L. You, Z. Wang, H. Li, J. Shou, Z. Jing, J. Xie, X. Sui, H. Pan, W. Han, The role of STAT3 in autophagy, Autophagy 11 (2015) 729–739.
[23] D.E. Johnson, R.A. O'Keefe, J.R. Grandis, Targeting the IL-6/JAK/STAT3 signalling axis in cancer, Nat. Rev. Clin. Oncol. 15 (2018) 234–248.
[24] D.R. Coleman, Ren, Z.P.K. Mandal, A.G. Cameron, G.A. Dyer, S. Muranjan, M. Campbell, X. Chen, J.S. McMurray, Investigation of the binding determinants of phosphopeptides targeted to the SRC homology 2 domain of the signal transducer and activator of transcription 3. Development of a high-affinity peptide inhibitor, J. Med. Chem. 48 (2005) 6661–6670.
[25] J. Chen, L. Bai, D. Bernard, Z. Nikolovska-Coleska, C. Gomez, J. Zhang, H. Yi, S. Wang, Structure-based design of conformationally constrained, cell-permeable STAT3 inhibitors, ACS Med. Chem. Lett. 2 (2010) 85–89.
[26] L. Lin, B. Hutzen, P.K. Li, S. Ball, M. Zuo, S. DeAngelis, E. Foust, M. Sobo, L. Friedman, D. Bhasin, L. Cen, C. Li, J. Lin, A novel small molecule, LLL12, inhibits STAT3 phosphorylation and activities and exhibits potent growth-suppressive activity in human cancer cells, Neoplasia 12 (2010) 39–50.
[27] L. Bai, H. Zhou, R. Xu, Y. Zhao, K. Chinnaswamy, D. McEachern, J. Chen, C.Y. Yang, Z. Liu, M. Wang, L. Liu, H. Jiang, B. Wen, P. Kumar, J.L. Meagher, D. Sun, J.A. Stuckey, S. Wang, A potent and selective small-molecule degrader of STAT3 achieves complete tumor regression in vivo, Canc. Cell 36 (2019) 498–511.
[28] A. Gelain, M. Mori, F. Meneghetti, S. Villa, Signal transducer and activator of transcription protein 3 (stat3): an update on its direct inhibitors as promising anticancer agents, Curr. Med. Chem. 26 (2019) 5165–5206.
[29] (a) Y. Li, H.A. Rogoff, S. Keates, Y. Gao, S. Murikipudi, K. Mikule, D. Leggett, W. Li, A.B. Pardee, C.J. Li, Suppression of cancer relapse and metastasis by inhibiting cancer stemness, Proc. Natl. Acad. Sci. U. S. A 112 (2015) 1839–1844;
(b) D.J. Jonker, L. Nott, T. Yoshino, S. Gill, J. Shapiro, A. Ohtsu, et al., Napabucasin versus placebo in refractory advanced colorectal cancer: a randomized phase 3 trial, Lancet Gastroenterol Hepatol 3 (2018) 263–270.
[30] C. Yoo, J. Kang, H.Y. Lim, J.H. Kim, M.-A. Lee, K.-H. Lee, T.-Y. Kim, B.-Y. Ryoo, Phase I dose-finding study of OPB-111077, a novel STAT3 inhibitor, in patients with advanced hepatocellular carcinoma, Cancer Res Treat 2 (2019) 510–518.
[31] (a) J.-X. Di, H.-Y. Zhang, C188-9, a small-molecule STAT3 inhibitor, exerts an antitumor effect on head and neck squamous cell carcinoma, Anti Canc. Drugs 8 (2019) 846–853.(b) ClinicalTrials.gov. https://clinicaltrials.gov/ct2/show/NCT03195699 (accessed 6 January 2021).
[32] M. Zhang, W. Zhu, Y. Li, Discovery of novel inhibitors of signal transducer and activator of transcription 3 (STAT3) signaling pathway by virtual screening, Eur. J. Med. Chem. 62 (2013) 301–310.
[33] T. Tei, Y. Sato, K. Hagiya, A. Tai, T. Okuyama, T. Sugimura, Chiral perturbation factor" approach reveals importance of entropy term in stereocontrol of the 2,4-pentanediol-tethered reaction, J. Org. Chem. 67 (2002) 6593–6598.
[34] S.F. Nielsen, S.B. Christensen, G. Cruciani, A. Kharazmi, T. Liljefors, Anti-leishmanial chalconesstatistical design, synthesis, and three-dimensional quantitative structure-activity relationship analysis, J. Med. Chem. 41 (1998) 4819–4832.
[35] A. Moreau, A. Couture, E. Deniau, P. Grandclaudon, S. Lebrun, First total synthesis of cichorine and zinnimidine, Org. Biomol. Chem. 3 (2005) 2305–2309.
[36] V. Guagnano, P. Furet, C. Spanka, V. Bordas, M.L. Douget, C. Stamm, J. Brueggen, M.R. Jensen, C. Schnell, H. Schmid, M. Wartmann, J. Berghausen, P. Drueckes, A. Zimmerlin, D. Bussiere, J. Murray, D.G. Porta, Discovery of 3-(2,6-dichloro-3,5-dimethoxy-phenyl)-1-{6-[4-(4-ethyl-piperazin-1-yl)-phenylamino]-pyrimidin-4-yl}-1-methyl-urea (NVP-BGJ398), a potent and selective inhibitor of the fibroblast growth factor receptor family of receptor tyrosine kinase, J. Med. Chem. 54 (2005) 7066–7083.
[37] P. Furet, G. Bold, T. Meyer, J. Roesel, V. Guagnano, Aromatic interactions with phenylalanine 691 and cysteine 828: a concept for FMS-like tyrosine kinase-3 inhibition. Application to the discovery of a new class of potential anti-leukemia agents, J. Med. Chem. 49 (2006) 4451–4454.
[38] M.S. Eom, J. Noh, H.S. Kim, S. Yoo, M.S. Han, M.S. Lee, High-Throughput screening protocol for the coupling reactions of aryl halides using a colorimetric chemosensor for halide ions, Org. Lett. 18 (2016) 1720–1723.
[39] M.R. Patel, A. Bhatt, J.D. Steffen, A. Chergui, J. Murai, Y. Pommier, J.M. Pascal, L.D. Trombetta, F.R. Fronczek, T.T. Talele, Discovery and structure-activity relationship of novel 2,3-dihydrobenzofuran-7-carboxamide and 2,3-dihydrobenzofuran-3(2H)-one-7-carboxamide derivatives as poly (ADP-ribose) polymerase-1 inhibitors, J. Med. Chem. 57 (2014) 5579–5601.
[40] S.S. Bisht, N. Dwivedi, V. Chaturvedi, N. Anand, M. Misra, R. Sharma, B. Kumar, R. Dwivedi, S. Singh, S.K. Sinha, V. Gupta, P.R. Mishra, A.K. Dwivedi, R.P. Tripathi, Synthesis and optimization of antitubercular activities in a series of 4-(aryloxy)phenyl cyclopropyl methanols, Eur. J. Med. Chem. 45 (2010) 5965–5978.
[41] P. Bamborough, H.A. Barnett, I. Becher, et al., GSK6853, a chemical probe for inhibition of the BRPF1 bromodomain, ACS Med. Chem. Lett. 7 (2016) 552–557.
[42] U. Bharadwaj, T.K. Eckols, M. Kolosov, M.M. Kasembeli, A. Adam, D. Torres, X. Zhang, L.E. Dobrolecki, W. Wei, M.T. Lewis, B. Dave, J.C. Chang, M.D. Landis, C.J. Creighton, M.A. Mancini, D.J. Tweardy, Drug-repositioning screening identified piperlongumine as a direct STAT3 inhibitor with potent activity against breast cancer, Oncogene 34 (2015) 1341–1353.
[43] T. Decker, P. Kovarik, Serine phosphorylation of STATs, Oncogene 19 (2000) 2628–2637.
[44] N. Kiuchi, K. Nakajima, M. Ichiba, T. Fukada, M. Narimatsu, K. Mizuno, M. Hibi, T. Hirano, STAT3 is required for the gp130-mediated full activation of the c-myc gene, J. Exp. Med. 189 (1999) 63–73.
[45] D. Puthier, R. Bataille, M. Amiot, IL-6 up-regulates mcl-1 in human myeloma cells through JAK/STAT rather than ras/MAP kinase pathway, Eur. J. Immunol. 29 (1999) 3945–3950.
[46] J. Schust, T. Berg, A high-throughput fluorescence polarization assay for signal transducer and activator of transcription 3, Anal. Biochem. 330 (2004) 114–118.
[47] J. Schust, B. Sperl, A. Hollis, T.U. Mayer, T. Berg, Stattic: a small-molecule inhibitor of STAT3 activation and dimerization, Chem. Biol. 13 (2006) 1235–1242.
[48] K. Feng, F. Wang, X. Shi, et al., Design, synthesis and biological evaluation of novel potent STAT3 inhibitors based on BBI608 for cancer therapy, Eur. J. Med. Chem. 201 (2020) 112428.
[49] J. Liu, Q. Zhang, Y. Ye, W. Li, J. Qiu, J. Liu, R. Zhan, W. Chen, Q. Yu Angoline, A selective IL-6/STAT3 signaling pathway inhibitor isolated from Zanthoxylum nitidum, Phytomedicine 21 (2014) 1088–1091.
[50] Q. Li, T. Zhang, S. Li, L. Tong, J. Li, Z. Su, F. Feng, D. Sun, Y. Tong, X. Wang, Z. Zhao, L. Zhu, J. Ding, H. Li, H. Xie, Y. Xu, Discovery of potent and noncovalent reversible EGFR kinase inhibitors of EGFR $^{L858R/T790M/C797S}$, ACS Med. Chem. Lett. 10 (2019) 869–873.
[51] Y. Saito, A. Azuma, K. Matsuda, K. Kamio, S. Abe, A. Gemma, Pirfenidone exerts a suppressive effect on CCL18 expression in U937-derived macrophages partly by inhibiting STAT6 phosphorylation, Immunopharmacol. Immunotoxicol. 38 (2016) 464–471.